Dominant-negative *SERPING1* variants cause intracellular retention of C1 inhibitor in hereditary angioedema

Didde Haslund,[1] Laura Barrett Ryø,[1] Sara Seidelin Majidi,[1] Iben Rose,[2] Kristian Alsbjerg Skipper,[1] Tue Fryland,[1,3] Anja Bille Bohn,[1] Claus Koch,[4] Martin K. Thomsen,[1,5] Yaseelan Palarasah,[4,6] Thomas J. Corydon,[1,7] Anette Bygum,[2] Lene N. Nejsum,[5] and Jacob Giehm Mikkelsen[1]

[1]Department of Biomedicine, Aarhus University, Aarhus, Denmark. [2]Department of Dermatology and Allergy Centre, Odense University Hospital, Odense C, Denmark. [3]iPSYCH, the Lundbeck Foundation Initiative for Integrative Psychiatric Research, Denmark. [4]Department of Cancer & Inflammation Research, University of Southern Denmark, Odense, Denmark. [5]Department of Clinical Medicine, Aarhus University, Aarhus, Denmark. [6]Unit for Thrombosis Research, Department of Regional Health Research, University of Southern Denmark and Department of Clinical Biochemistry, Hospital of South West Jutland, Esbjerg, Denmark. [7]Department of Ophthalmology, Aarhus University Hospital, Aarhus, Denmark.

Hereditary angioedema (HAE) is an autosomal dominant disease characterized by recurrent edema attacks associated with morbidity and mortality. HAE results from variations in the *SERPING1* gene that encodes the C1 inhibitor (C1INH), a serine protease inhibitor (serpin). Reduced plasma levels of C1INH lead to enhanced activation of the contact system, triggering high levels of bradykinin and increased vascular permeability, but the cellular mechanisms leading to low C1INH levels (20%–30% of normal) in heterozygous HAE type I patients remain obscure. Here, we showed that C1INH encoded by a subset of HAE-causing *SERPING1* alleles affected secretion of normal C1INH protein in a dominant-negative fashion by triggering formation of protein-protein interactions between normal and mutant C1INH, leading to the creation of larger intracellular C1INH aggregates that were trapped in the endoplasmic reticulum (ER). Notably, intracellular aggregation of C1INH and ER abnormality were observed in fibroblasts from a heterozygous carrier of a dominant-negative *SERPING1* gene variant, but the condition was ameliorated by viral delivery of the *SERPING1* gene. Collectively, our data link abnormal accumulation of serpins, a hallmark of serpinopathies, with dominant-negative disease mechanisms affecting C1INH plasma levels in HAE type I patients, and may pave the way for new treatments of HAE.

Introduction

Hereditary angioedema (HAE) is a rare autosomal dominant genetic disease with an estimated prevalence of 1:50,000 to 1:70,000 worldwide (1–3). HAE is characterized by recurrent nonpitting edema attacks of the deep dermis, submucosa, and subcutaneous tissues. Attacks often involve the extremities, the face, the gastrointestinal tract, and less frequently, but potentially life-threatening, the larynx (4). If not fatal, these very painful attacks are self-limiting and last up to 5 days.

HAE is caused by variants of the serpin family G member 1 (*SERPING1*) gene encoding the serine protease inhibitor (serpin) C1 inhibitor (C1INH) (5). To date, more than 450 different HAE-causing *SERPING1* gene variants have been identified, leading to either low levels (in the case of HAE type I) or reduced function (in the case of HAE type II) of C1INH (2, 6). HAE with a normal C1INH level (HAE-nC1INH), in contrast, is reported to be caused by mutations in genes encoding other proteins, including factor XII (7), plasminogen (8), and angiopoietin 1 (9).

C1INH belongs to the largest and most diverse superfamily of protease inhibitors, the serpin superfamily (10), which also includes α1-antitrypsin (A1AT) and antithrombin. Serpins play a critical role in the control of proteases involved in blood coagulation as well as in inflammatory, complement, and fibrinolytic pathways (11, 12), and their importance as crucial regulators of protease activity is emphasized by the number and severity of diseases caused by serpin dysfunction. Serpins share a highly conserved tertiary core structure (Figure 1A) comprised of 3 β-sheets (sA, sB, and sC), 8 or 9 α-helices (termed hA-hI), and a protruding reactive center loop (RCL) (13). In native serpins, the RCL, located outside the tertiary core of the serpin, forms a flexible stretch of approximately 20 amino acids, which provides structural flexibility in a solvent-exposed environment (14). The amino acid sequence of the RCL is numbered P17 (N-terminal) to P3′ (C-terminal). The peptide bond between P1 and P1′, referred to as the scissile bond, mimics the natural substrate and thus serves as a bait region for binding and cleavage of the targeted protease (15, 16). The protruding structure of the RCL makes it more accessible for interaction with target proteases, but it also causes the native serpin to be in a metastable form.

▶ Related Commentary: p. 66

Conflict of interest: The authors have declared that no conflict of interest exists.

Submitted: November 30, 2017; **Accepted:** October 30, 2018.
Reference information: *J Clin Invest*. 2019;129(1):388–405.
https://doi.org/10.1172/JCI98869.

When a target protease recognizes and cleaves the scissile bond, the RCL domain inserts into the central sA β-sheet as an additional strand and drags the covalently bound protease to the base of the serpin molecule (17, 18). After this dramatic conformational change, the serpin adopts a highly stable conformation, leading to irreversible inhibition of the protease (17).

Metastability of native serpins is a driving force for their inhibitory mouse-trap function, but also renders serpins prone to polymerization (11). This tendency to form polymers can be further induced by mutations affecting the serpin structure and function, leading potentially to dysfunction and diseases collectively referred to as serpinopathies (10, 13). Formation of serpin polymers are known to cause disease in patients with α1-antitrypsin deficiency (A1ATD) (19) and familial encephalopathy with neuroserpin inclusion bodies (FENIBs) (20). According to the loop-sheet A model, the most widely accepted model of polymer formation among serpins, long-chain serpin polymers are formed due to the capacity of the RCL of one serpin to dock into the sA of another serpin (21). Polymers of this type consisting of A1AT Z-variant subunits (Glu342Lys) (21) accumulate in the rough endoplasmic reticulum (ER) of hepatocytes and cause cell death and liver cirrhosis in patients with A1ATD (22). Most serpinopathy-causing serpin defects are located, like the A1AT Z-variant, in the breach and shutter domains (Figure 1A) involved in facilitating the initial insertion of the RCL into the sA and accepting the RCL during protease inhibition, respectively. Thus, it is hypothesized that defects within the breach and shutter domains destabilize and open the sA, thereby allowing the RCL of other serpins to dock into this domain (19). Notably, polymers of C1INH protein have been detected in plasma isolated from HAE type I patients (23), but it remains unclear whether C1INH polymer formation occurs intracellularly and to what extent polymers affect the pathogenesis of HAE.

C1INH has central regulatory functions in several pathways that are part of the complement system, the fibrinolytic system, and the contact system. Under normal physiological conditions, C1INH regulates the contact system by inhibiting the activity of the 2 serine proteases FXIIa and kallikrein (24). However, the very low C1INH plasma level in HAE type I patients results in a poorly regulated contact pathway. It is widely accepted that enhanced activation of the contact system, leading to increased generation of the vasoactive peptide bradykinin, is a key trigger of the edema attacks observed in HAE patients (24, 25). Bradykinin formed in the contact system acts through the G-protein–coupled bradykinin B2 receptor on the surface of endothelial cells and causes increased vascular permeability and vasodilation resulting in edema formation (5). C1INH is produced mainly in hepatocytes, reaching in healthy individuals a plasma concentration of 0.21–0.39 g/l (26). Of note, C1INH can be produced and secreted from other cell types like peripheral blood monocytes, fibroblasts, and endothelial cells (27).

The majority of HAE patients are heterozygous carriers of a mutated *SERPING1* allele, resulting in production of functional C1INH only from a single allele. However, in most HAE type I patients the C1INH plasma level is reduced markedly below the expected level, often to around 20% of normal (28). These findings may potentially reflect an inhibitory role of mutated C1INH protein on C1INH protein derived from the WT *SERPING1* allele, but mechanisms explaining such trans-inhibition have not been described. It has been suggested that the defective allele inhibits the synthesis of normal C1INH (29), but evidence of a dominant-negative action of mutated C1INH protein in the pathology of HAE is still lacking.

In this report, we demonstrate reduced cellular secretion of mutated C1INH protein expressed from alleles identified in patients with HAE type I. Our findings provide evidence, to our knowledge for the first time, that C1INH encoded from HAE-causing *SERPING1* alleles can act upon C1INH expressed from the WT *SERPING1* allele in a dominant-negative fashion, triggering the formation of intracellular C1INH aggregates and a resulting drop in the secretion of functional C1INH. Notably, such phenotypes are evident in skin-derived fibroblasts from patients carrying the most severe dominant-negative allele. Collectively, our data indicate that reduced levels of C1INH leading to HAE type I are caused, in a subset of patients, by abnormal C1INH protein aggregation induced by mutated C1INH. Importantly, in patient-derived fibroblasts, the secretion barrier can be overcome by administration of the WT *SERPING1* gene, suggesting that dominant-negative disease mechanisms can be overcome by gene supplementation, providing hope for future development of gene therapies for HAE.

Results

Reduced C1INH plasma levels in HAE type I patients carrying SERPING1 gene variants encoding full-length or near full-length C1INH. Most HAE type I patients are heterozygous for mutations in the *SERPING1* gene and maintain production of functional C1INH only from a single WT *SERPING1* allele. However, the reduced plasma C1INH level in patients diagnosed with HAE type I suggests that the C1INH level in the blood of HAE patients is affected by mechanisms contributing to development of the disease. This led us to hypothesize that dominant-negative effects of the disease allele are evident intracellularly and directly involved in restricting C1INH secretion leading to HAE type I. To investigate if such mechanisms contribute to reduced plasma C1INH levels in HAE type I patients, we initially investigated a total of 6 HAE type I–causing *SERPING1* gene variants present in Danish HAE patients. As we reasoned that disease alleles encoding full-length or near full-length C1INH proteins were most likely to have a dominant-negative effect, we excluded disease alleles giving rise to mRNA degradation and variants with gross gene rearrangements from our analysis, and gene variants for which premature stop codons were not introduced and the reading frame was not affected were selected (c.550G>A, c.551_685del, c.566C>A, c.838_846del, c.1417G>A, and c.1427C>T; Figure 1B and Supplemental Table 1; supplemental material available online with this article; https://doi.org/10.1172/JCI98869DS1). The location of each of these amino acid substitutions and deletions in the predicted 3D structure of C1INH is indicated in Figure 1A. Among the 6 patients carrying each of these *SERPING1* gene variants, 5 showed severely reduced levels of plasma C1INH ranging from 0.05–0.13 g/l, whereas the remaining patient had a plasma concentration of 0.2 g/l (Figure 1B).

Reduced secretion of mutated C1INH protein from transfected cells. To investigate the functional properties of the selected panel of HAE type I–causing *SERPING1* gene variants, we initially

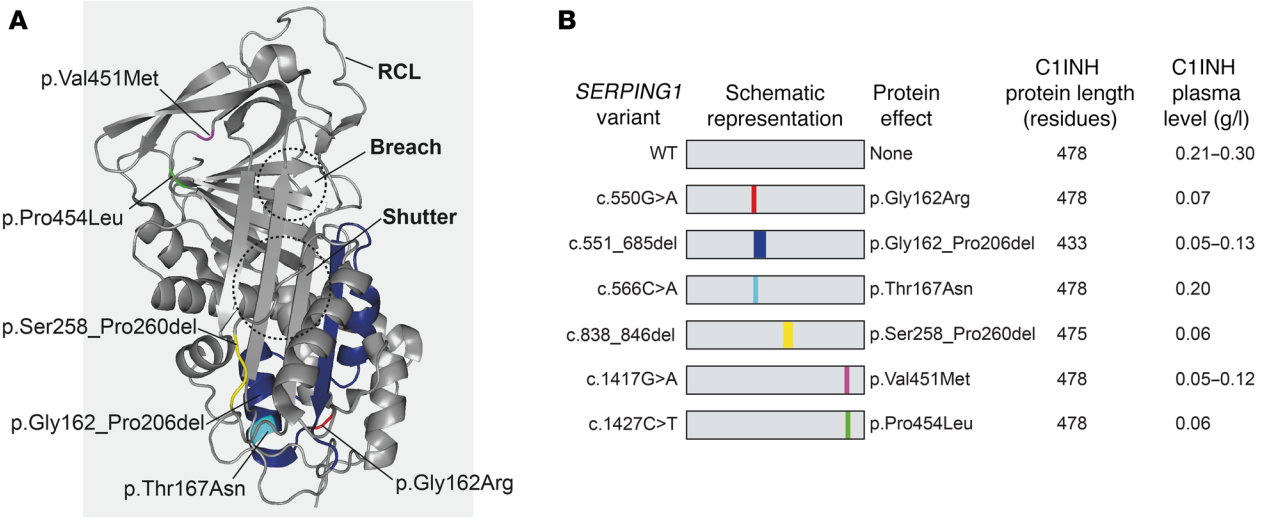

Figure 1. Characteristics of studied *SERPING1* gene variants and plasma levels of C1INH in patients carrying the variants. (**A**) The overall structure of active C1INH protein (Protein Data Bank entry 5DU3). The locations of the studied HAE-causing variants are marked as follows: p.Gly162Arg (red), p.Thr167Asn (cyan), p.Val451Met (magenta) and p.Pro454Leu (green). For p.Gly162_Pro206del and p.Ser258_Pro260del the areas deleted in C1INH are marked with dark blue and yellow, respectively. (**B**) Presentation of the 6 studied *SERPING1* gene variants and key data related to each gene variation and to patients carrying the variants. See Supplemental Table 1 for additional information.

established a cellular model system based on ectopic expression of normal and mutated C1INH variants. First, a panel of expression vectors encoding the different *SERPING1* gene variants was constructed (referred to as pSERPING1[Variant], by which the type of mutation is indicated within the brackets) (Figure 2A). Since C1INH is primarily produced in and secreted from the liver, we carried out expression experiments in HepG2 cells, a human hepatocarcinoma cell line. Initially, HepG2 cells were individually transfected with the 7 different C1INH expression constructs (6 mutated variants and the WT *SERPING1* control), and the amount of C1INH secreted into the medium was measured by sandwich ELISA. Also, untransfected cells or cells transfected with an empty vector were included as negative controls. The concentration of C1INH was 1,600 ± 240 ng/ml in medium from cells transfected with pSERPING1[WT], whereas secretion of C1INH from cells transfected with plasmid expressing HAE-causing *SERPING1* gene variants was severely reduced resulting in background levels for several of the variants (Figure 2B). To verify that the reduced C1INH secretion from cells expressing HAE-causing *SERPING1* variants was due to impaired C1INH secretion and not insufficient C1INH expression, we generated a new set of vectors in which the different *SERPING1* gene variants were fused to a human influenza hemagglutinin (HA) tag (pSERPING1[Variant]-HA) (Figure 2A), allowing evaluation of both secreted and intracellular C1INH-HA levels by Western blotting. As shown in Figure 2C (quantification in Supplemental Figure 1A), only cells transfected with pSERPING1[WT]-HA were capable of secreting C1INH into the medium to a level that was detectable. Notably, intracellular HA-tagged C1INH was detectable in all cell samples transfected with HAE-causing *SERPING1* gene variants, demonstrating that the HAE-causing variants were indeed expressed after transfection. Interestingly, for all variants we noted that the levels of intracellular HA-tagged C1INH were increased, for 3 of the variants 2-fold or more, relative to the positive control (Figure 2C, Supplemental Figure 1B), suggesting that reduced secretion of C1INH correlated with increased intracellular accumulation of the protein.

To establish an experimental platform allowing us to distinguish normal from mutated C1INH and further assess cellular C1INH processing pathways, we set out to generate a new set of expression vectors, in which the different *SERPING1* gene variants were fused to a sequence encoding fluorescent mCherry protein (Figure 2A). Ectopic production of C1INH carrying a fluorescent mCherry tag enabled analyses of both the intracellular level and the secretion of C1INH from the same cells by measuring the fluorescence intensity in cells and medium, respectively. To certify that the mCherry tag did not itself hinder C1INH secretion, we confirmed by ELISA that mCherry-tagged normal C1INH was indeed robustly secreted from plasmid-transfected HepG2 cells, reaching levels of 240 ± 6 ng/ml in the medium (Figure 2D). Clearly, the level of detectable C1INH carrying the mCherry tag was lower than the level obtained with untagged C1INH (Figure 2B), which may reflect reduced detection using the C1INH antibody, reduced expression or stability of the protein, posttranslational events affecting transport or secretion, or potentially a combination of these effects. As expected, we did not detect any C1INH protein in medium from cells transfected with plasmid encoding the HAE-causing *SERPING1* gene variants (Figure 2D).

We then transfected HepG2 cells with the different pSERPING1[Variant]-mCherry vectors and determined secreted and intracellular levels of mCherry-tagged C1INH by measuring the fluorescence intensity. Using this approach, the amount of C1INH-mCherry secreted into the medium from cells transfected with the 6 HAE-causing *SERPING1* gene variants was found to be markedly reduced compared with cells transfected with pSERPING1[WT]-mCherry (Figure 2E), confirming our previous findings. Importantly, for all 6 variants increased intracellular

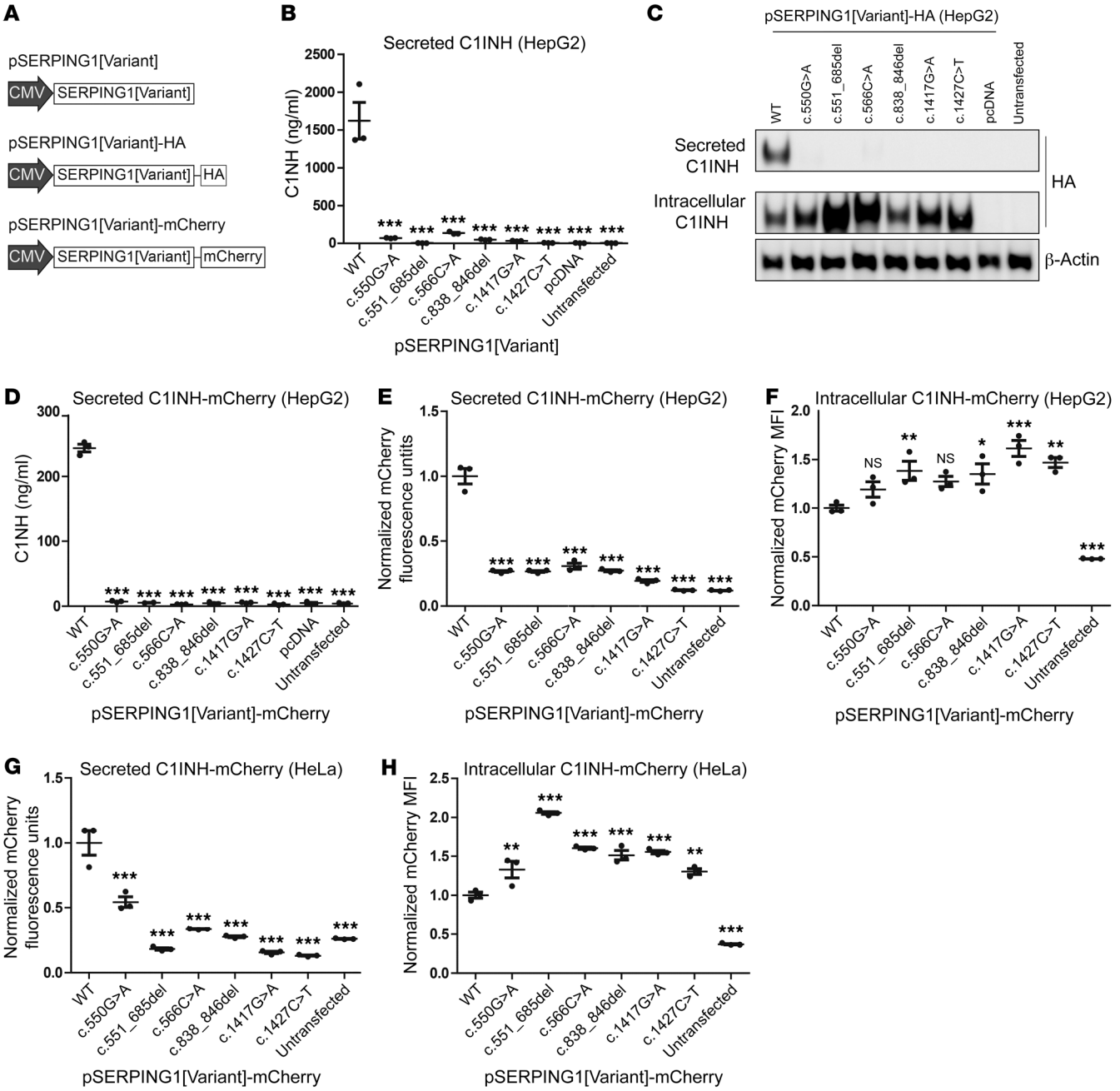

Figure 2. Expression and severely reduced secretion of C1INH encoded by the 6 studied *SERPING1* gene variants. (**A**) Schematic representation of the vector types used in this study to express *SERPING1* gene variants. Black arrows indicate the promoter derived from cytomegalovirus (CMV). (**B**) C1INH levels in medium from HepG2 cells transfected with 900 ng pSERPING1[Variant] measured by ELISA. (**C**) Western blot analysis of medium protein and total protein derived from HepG2 cells transfected with 900 ng pSERPING1[Variant]-HA. The secreted and intracellular C1INH levels were detected using a HA-specific antibody. (**D**) C1INH levels in medium from HepG2 cells transfected with 900 ng pSERPING1[Variant]-mCherry measured by ELISA. (**E** and **F**) Secreted and intracellular levels of C1INH in HepG2 cells measured by mCherry fluorescence intensity. (**G** and **H**) Secreted and intracellular levels of C1INH in HeLa cells measured by mCherry fluorescence intensity. Cells were transfected with different pSERPING1[Variant]-mCherry vectors. The amount of C1INH-mCherry secreted into the medium was determined using a fluorescence scanner (**E** and **G**) and the intracellular level by flow cytometry (**F** and **H**). (**B**–**H**) Transfections were carried out in triplicate ($n = 3$) and similar results were seen in at least 2 independent experiments. Data are mean ± SEM. $^*P < 0.05$, $^{**}P < 0.01$, $^{***}P < 0.001$, compared with WT. Statistical analyses were performed by 1-way ANOVA with Dunnett's multiple comparison test. MFI, median fluorescence intensity.

C1INH-mCherry levels relative to the control were measured by flow cytometry (Figure 2F), indicating that the low level of secretion of mutated C1INH correlated with increased intracellular accumulation and thus did not reflect reduced expression of C1INH. We performed a similar experiment in HeLa cells with a higher transfection efficacy and confirmed reduced secretion and increased intracellular accumulation of disease-causing C1INH variants also in these cells (Figure 2, G and H). We noted

that this specific phenotype in HeLa cells was particularly severe for the c.551_685del variant.

Defective C1INH variants induce impaired secretion and enhanced intracellular accumulation of coexpressed normal C1INH. To model the coexpression of 2 *SERPING1* alleles in HAE type I patients, we took advantage of mCherry-tagged C1INH protein variants using the approach schematically depicted in Figure 3A. To evaluate the effect of mutated C1INH on secretion and intracellular accumulation as well as on localization of normal C1INH tagged with mCherry, HepG2 and HeLa cells were transfected with equal amounts of pSERPING1[WT]-mCherry and vectors encoding HAE-causing *SERPING1* gene variants (pSERPING1[Variant]). First, we found that secreted levels of normal C1INH-mCherry were reduced in medium from cells simultaneously expressing 1 of the 6 defective C1INH variants relative to cells cotransfected with pcDNA as a negative control (Figure 3B). We also found that coexpression of normal C1INH-mCherry with normal C1INH resulted in this assay in increased secretion of mCherry-tagged C1INH protein. Next, in concordance with reduced secretion, we measured an increase in the intracellular level of normal C1INH-mCherry in all cultures expressing the HAE-causing *SERPING1* gene variants compared with control cells (Figure 3C), supporting the notion that the examined defective C1INH variants interfered with secretion of coexpressed normal C1INH-mCherry and thus induced intracellular accumulation of mCherry-tagged normal C1INH. Once again, the c.551_685del variant was found to induce the most severe accumulation phenotype (Figure 3C). In HeLa cells, similar cotransfection experiments showed reduced secretion of normal C1INH-mCherry only in cells coexpressing C1INH from pSERPING1[c.551_685del] (Figure 3D), whereas increased intracellular levels of C1INH-mCherry were evident 72 hours after transfection for 4 of the 6 *SERPING1* expression constructs (c.550G>A; c.551_685del; 566C>A; c.838_846del) with c.551_685del and 566C>A *SERPING1* variants causing the highest levels of protein accumulation (Figure 3E). In summary, these findings suggest that HAE-causing *SERPING1* gene variants encode C1INH that restricts secretion of functional C1INH and thus induces cellular phenotypes in a dominant-negative fashion.

To evaluate the strength of mutated C1INH as a dominant-negative inhibitor, we carried out a dose-response experiment with the c.551_685del variant, which seemed to show the most profound phenotype. By cotransfection of HeLa cells with pSERPING1[WT]-mCherry (450 ng) and increasing amounts of pSERPING1[c.551_685del] (50, 200, 450, 700, or 900 ng), a gradual decrease of normal C1INH-mCherry secretion with increasing amounts of plasmid encoding defective C1INH was observed (Figure 3F). In accordance, flow cytometry analysis of transfected cells showed gradually increased levels of intracellular C1INH-mCherry (Figure 3G), indicating that cellular transport and secretion of C1INH-mCherry was massively blocked by defective C1INH protein. In contrast, in control samples cotransfected with pSERPING1[WT], C1INH-mCherry secretion was enhanced with increasing amounts of plasmid, whereas intracellular levels were unaffected (Figure 3, F and G). In summary, our data suggest that C1INH variants expressed in HAE patients act as dominant-negative inhibitors inducing intracellular accumulation and reduced secretion of functional C1INH.

Intracellular congestion of normal C1INH induced by HAE-causing C1INH variants. Using the model system based on mCherry-tagged C1INH, we moved on to investigate the intracellular localization of C1INH by live widefield microscopy. Due to the small size of HepG2 rendering these cells unsuitable for microscopy-based analysis, we performed these analyses in HeLa cells. First, intracellular localization of the different C1INH-mCherry variants was visualized in HeLa cells transfected with the different pSERPING1[Variant]-mCherry vectors. As seen in Figure 4A, C1INH-mCherry derived from pSERPING1[WT]-mCherry was evenly distributed throughout the entire cell almost in a reticular pattern. Out of the 6 HAE-causing *SERPING1* gene variants, the cellular C1INH-mCherry pattern was clearly altered only in cells transfected with pSERPING1[c.566C>A]-mCherry (encoding $C1INH_{Thr167Asn}$-mCherry) relative to cells transfected with pSERPING1[WT]-mCherry (Figure 4A). In these cells, we observed accumulation of $C1INH_{Thr167Asn}$-mCherry in patterns reminiscent of localized aggregates, correlating with the low levels of C1INH secretion and increased intracellular accumulation observed previously for this variant (Figure 2, G and H).

To investigate whether the mutated C1INH variants in a dominant-negative fashion induced formation of intracellular aggregates containing coexpressed normal C1INH-mCherry protein, HeLa cells were cotransfected in a series of transfections with pSERPING1[WT]-mCherry and vectors encoding each of the HAE-causing *SERPING1* gene variants (pSERPING1[Variant]). Notably, relative to the controls, marked changes in the intracellular distribution of normal C1INH-mCherry were evident in cells coexpressing the c.550G>A, c.551_685del, and c.566C>A *SERPING1* variants, respectively (Figure 4B). For all 3 variants, the emergence of a number of well-defined fluorescent foci unveiled a very distinct cellular phenotype, which was, over several experiments, reproducibly most severe in cells expressing $C1INH_{Gly162\_Pro206del}$ encoded by pSERPING1[c.551_685del]. As this phenotype correlated well with the reduced secretion and dominant-negative effects of this variant, we intensified the analysis of this particular *SERPING1* allele.

Next, we addressed whether the formation of fluorescent foci could potentially be an artifact of overexpressing $C1INH_{Gly162\_Pro206del}$. To evaluate whether there was a correlation between the formation of C1INH-mCherry aggregates and the amount of mutant protein, cells were cotransfected with a fixed amount of pSERPING1[WT]-mCherry and increasing amounts of pSERPING1[c.551_685del], or pSERPING1[WT] as a control. Even with increased amounts of pSERPING1[WT], we did not observe formation of C1INH-containing foci (Supplemental Figure 2A). In contrast, even with the lowest amount of pSERPING1[c.551_685del], fluorescent foci were firmly generated, and formation of foci did not seem to be further boosted with increasing dosages of transfected plasmid (Supplemental Figure 2B). Together, these findings showed that the formation and size of intracellular C1INH aggregates was not directly correlated to the amount of protein and that the abnormal cellular phenotype did not originate from massive overproduction of the inhibitory protein.

Prominent intracellular C1INH focus formation induced by $C1INH_{Gly162\_Pro206del}$ as quantified by Imagestream analysis. To evaluate the prevalence of the cellular C1INH aggregation phenotype observed in cells coexpressing normal C1INH and $C1INH_{Gly162\_Pro206del}$, we set out to quantify formation of fluorescent

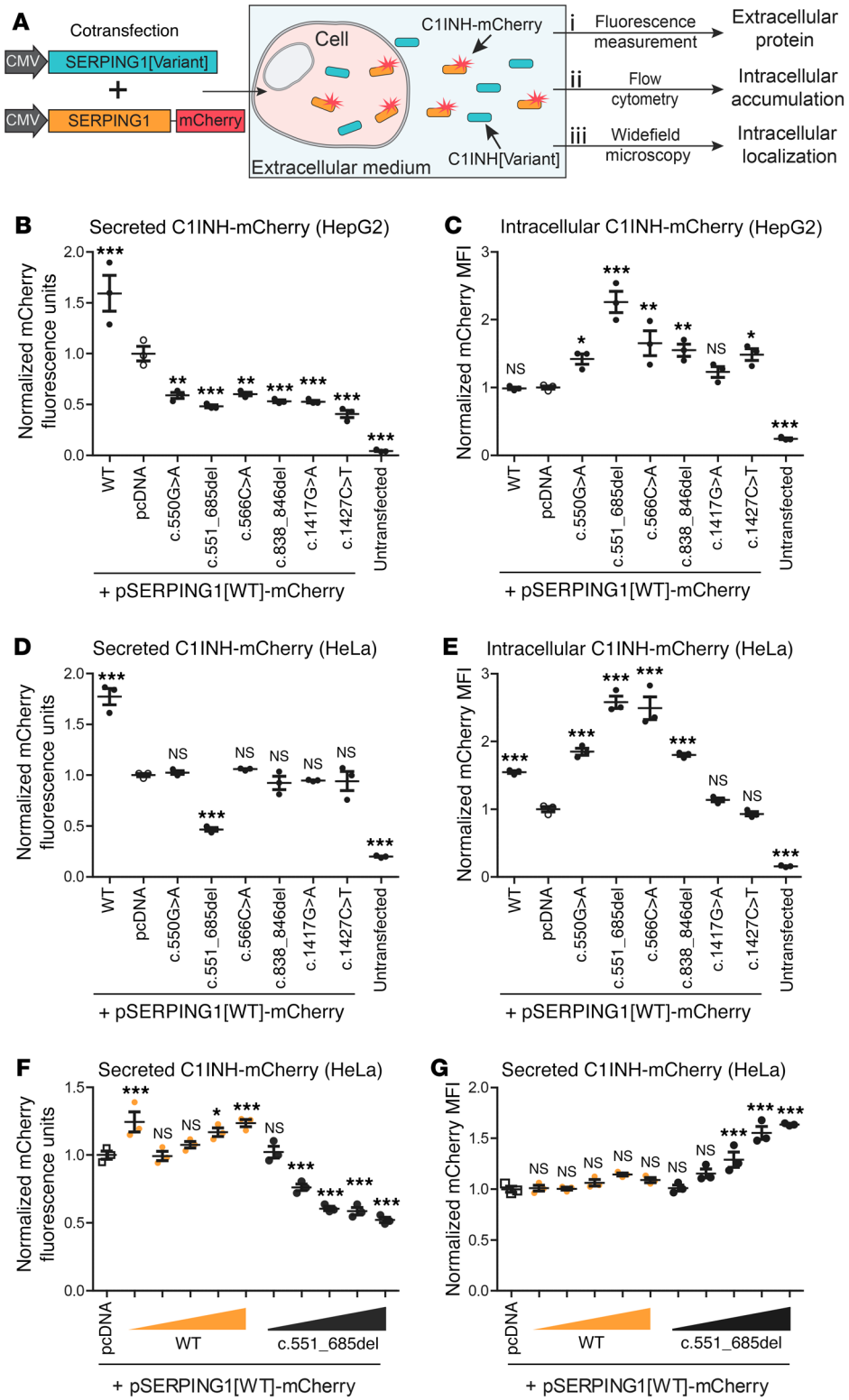

Figure 3. Negative impact of C1INH encoded by HAE-causing *SERPING1* gene variants on secretion of normal C1INH-mCherry correlates with increased intracellular protein levels. (**A**) Schematic representation of the cellular assay system. Cells were cotransfected with pSERPING1[Variant] and pSERPING1[WT]-mCherry. Expression of mCherry-fused normal C1INH allowed evaluation of the effect of different *SERPING1* gene variants on (i) secretion, (ii) intracellular retention, and (iii) intracellular localization of normal C1INH-mCherry. (**B** and **C**) Levels of secreted and intracellular C1INH-mCherry in HepG2 cells cotransfected with 450 ng of both pSERPING1[Variant] and pSERPING1[WT]-mCherry. (**D** and **E**) Levels of secreted and intracellular C1INH-mCherry in HeLa cells transfected as in **B** and **C**. Secretion of normal C1INH-mCherry was measured by fluorescence scanning (**B** and **D**) and the intracellular level by flow cytometry (**C** and **E**). (**F**) Increasingly restricted C1INH secretion with higher levels of mutant C1INH. Dose-response experiment was carried out in HeLa cells. Cells were cotransfected with 450 ng pSERPING1[WT]-mCherry and 50, 200, 450, 700, or 900 ng pSERPING1[WT] or pSERPING1[c.551_685del]. pcDNA plasmid was included in all transfections to ensure a total amount of 1,350 ng plasmid DNA in each transfection reaction. (**G**) Intracellular levels of C1INH-mCherry in cells described in **F**. (**B**–**G**) Transfections were carried out in triplicate ($n = 3$) and similar results were seen in at least 3 independent experiments. Data are mean ± SEM. $^*P < 0.05$, $^{**}P < 0.01$, $^{***}P < 0.001$, compared with pcDNA. Statistical analyses were performed by 1-way ANOVA with Dunnett's multiple comparison test. MFI, median fluorescence intensity.

foci using Imagestream technology (30), allowing high-resolution microscopy and computational analysis of thousands of cells expressing C1INH-mCherry. HeLa cells were cotransfected with pSERPING1[WT]-mCherry and either pcDNA, pSERPING1[WT], or pSERPING1[c.551_685del]. Untransfected cells were included as a negative control. We analyzed 20,000 cells from each cotransfection (Figure 4C). The number of mCherry-positive cells in each group ranged between 1,395 and 3,579, with zero mCherry-positive cells in the negative control. The percentage of cells with accumulation of C1INH-mCherry protein in the cell perimeter was defined using the maximum contour position feature describing the location of high-intensity C1INH-mCherry protein. The position was represented by a number between 0 and 1, with 0 being the center of the cell

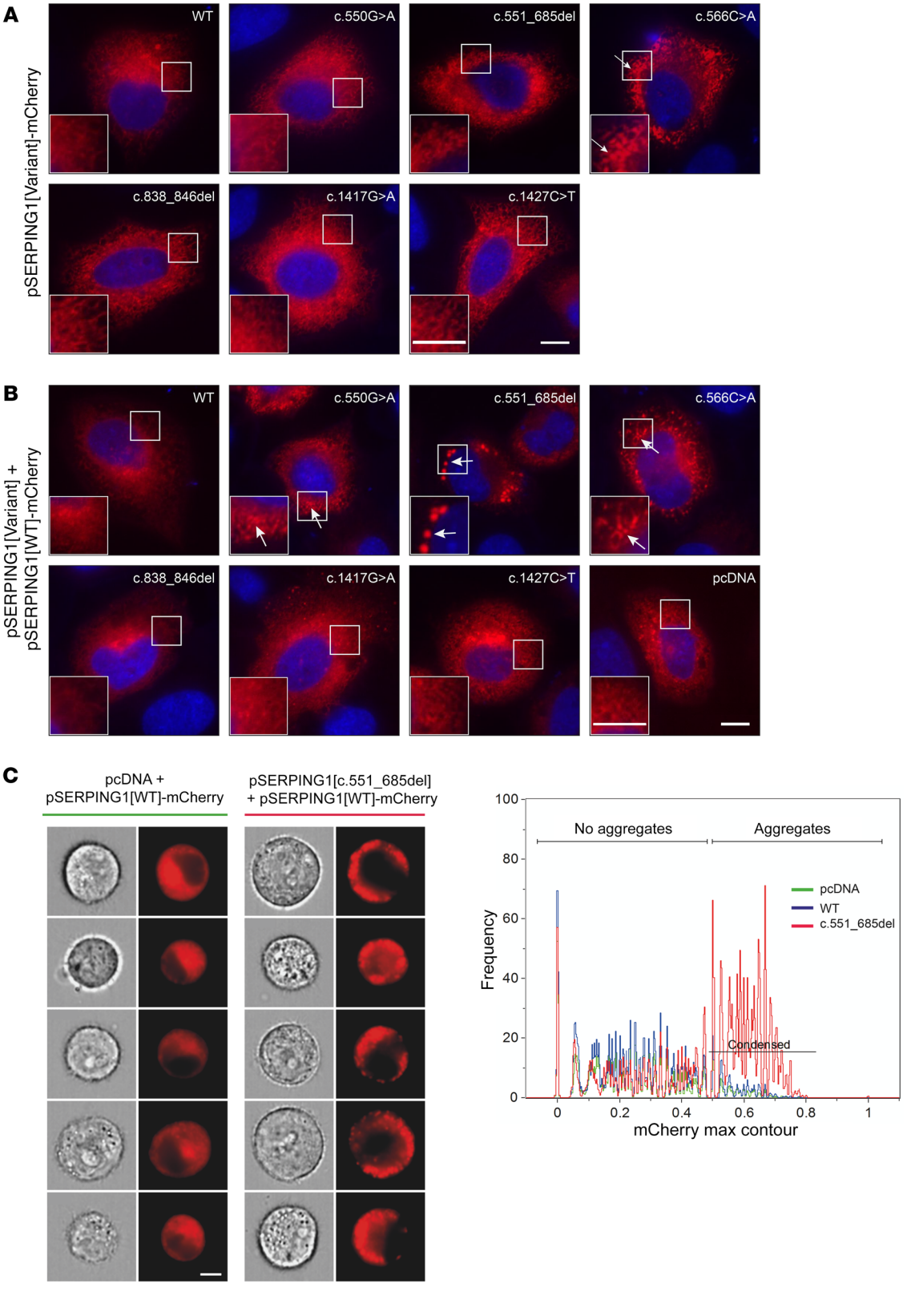
A
pSERPING1[Variant]-mCherry
WT
c.550G>A
c.551_685del
c.566C>A
c.838_846del
c.1417G>A
c.1427C>T
B
pSERPING1[Variant] + pSERPING1[WT]-mCherry
WT
c.550G>A
c.551_685del
c.566C>A
c.838_846del
c.1417G>A
c.1427C>T
pcDNA
C
pcDNA + pSERPING1[WT]-mCherry
pSERPING1[c.551_685del] + pSERPING1[WT]-mCherry
No aggregates
Aggregates
pcDNA
WT
c.551_685del
Condensed
Frequency
mCherry max contour
0
20
40
60
80
100
0
0.2
0.4
0.6
0.8
1

Figure 4. Intracellular localization of C1INH-mCherry detected by widefield microscopy and Imagestream analysis. (**A**) Intracellular localization of normal and mutated C1INH-mCherry (red). Live widefield microscopy of HeLa cells cultured for 48 hours after transfection with 900 ng pSERPING1[Variant]-mCherry. Scale bar: 10 μm. (**B**) Intracellular localization of normal C1INH-mCherry (red) in the presence of HAE-causing *SERPING1* gene variants. Live widefield microscopy of HeLa cells cultured for 48 hours after cotransfection with 450 ng pSERPING1[WT]-mCherry (red) and 450 ng pSERPING1[Variant] gene variants. Aggregates of normal C1INH-mCherry were detectable in cells cotransfected with pSERPING1[WT]-mCherry and vectors encoding the following *SERPING1* variants: c.550G>A, c.551_685del, or c.566C>A. Examples of aggregates are indicated with white arrows. Cells were incubated with Hoechst to visualize nuclei (blue). Scale bar: 10 μm. (**C**) High prevalence of C1INH aggregates in cells expressing normal and c.551_685del *SERPING1* gene variants. HeLa cells were cotransfected with pSERPING1[WT]-mCherry and either pcDNA, pSERPING1[WT] or pSERPING1[c.551_685del]. The cells were analyzed by imaging flow cytometry using Imagestream technology, and cells with C1INH aggregates were identified to have a max contour above 0.5 (condensed). Two sets of columns (left panels) show light/fluorescence microscopy images of cells expressing SERPING1[WT]-mCherry in the presence of pcDNA and pSERPING1[c.551_685del], respectively. Scale bar: 7 μm. Right panel: Imagestream-based quantification of larger cell populations, showing aggregate formation predominantly in cells cotransfected with pSERPING1[WT]-mCherry and pSERPING1[c.551_685del] (red graph). Number (*n*) of condensed cells relative to the number of mCherry-positive cells were as follows: pSERPING1[WT]-mCherry + pcDNA, *n* = 262/2,137; pSERPING1[WT]-mCherry + pSERPING1[WT], *n* = 159/1,395; pSERPING1[WT]-mCherry + pSERPING1[c.551_685del], *n* = 2,115/3,579. Data shown in **A** and **B** are representative of findings from more than 3 biological replicates, and similar results were seen in at least 3 independent experiments. Imaging flow cytometry in **C** was performed twice with reproducible results.

and 1 being the perimeter of the cell. By visual inspection of the generated cell images, foci of normal C1INH-mCherry were prevalent in cells with a maximum contour position above 0.5 (condensed gate in Figure 4C, right panel). In the mCherry-positive cells cotransfected with pSERPING1[WT]-mCherry and either pcDNA or pSERPING1[WT], 11.4% and 12.3%, respectively, had a maximum contour position above 0.5. In contrast, 59.1% of the mCherry-positive cells cotransfected with pSERPING1[WT]-mCherry and pSERPING1[c.551_685del] had a maximum contour position above 0.5 (condensed gate, Figure 4C), emphasizing that the inclusion of normal C1INH in larger aggregate-like formations was induced when $C1INH_{Gly162\_Pro206del}$ was coexpressed in transfected cells.

Blockage of accumulated C1INH within the ER. It is widely accepted that aggregation of serpin polymers within the ER is part of the pathology of serpinopathies like α1-antitrypsin deficiency (20). To investigate if aggregates of normal C1INH induced by defective C1INH protein indeed accumulated within the ER, HeLa cells were cotransfected with equal amounts of pSERPING1[WT]-HA and pcDNA, pSERPING1[WT], or pSERPING1[c.551_685del] (Figure 5). To visualize ER in subsequent microscopy analyses, an expression plasmid encoding a Tomato fluorescence gene fused to an ER-targeting sequence was included in the transfections. By staining for HA-tagged normal C1INH, we observed a diffuse distribution pattern, suggesting that normal C1INH colocalized with ER in cells cotransfected with pcDNA or pSERPING1[WT] (Figure 5, upper 2 rows). Aggregate-like structures containing normal C1INH-HA formed in the presence of pSERPING1[c.551_685del] and clearly accumulated within the ER (Figure 5, bottom row). Interestingly, in contrast to the reticular-like ER structure observed in cells cotransfected with pcDNA or pSERPING1[WT], the ER structure underwent dramatic alterations in cells cotransfected with pSERPING1[c.551_685del], showing a constipated ER structure adapting the shape of the C1INH-HA foci. Of note, using an alternative approach by which ER in HeLa cells was visualized with an antibody recognizing the KDEL motif, we observed the same phenomenon in cells cotransfected with pSERPING1[WT]-mCherry and pSERPING1[c.551_685del] (Supplemental Figure 3). Collectively, these findings suggested that $C1INH_{Gly162\_Pro206del}$ inhibits the secretion of C1INH in a dominant-negative fashion by inducing accumulation of normal C1INH in the ER. As this phenotype showed pronounced similarity to cellular phenotypes suggested to cause α1-antitrypsin deficiency (A1ATD), our results prompted us to validate and compare aggregation of the 2 serpins in our cellular model system based on fusing serpins to mCherry.

In A1ATD caused by the frequent Z variant of the *SERPINA1* gene, the plasma level of α1-antitrypsin is significantly reduced in patients who are homozygous for the Z variant compared with healthy individuals carrying 2 normal SERPINA1 alleles (referred to as M alleles) (19). To mimic this scenario, HeLa cells were transfected with vectors encoding either an mCherry-tagged M or Z SERPINA1 cDNA variant (pSERPINA1[Variant]-mCherry), and the secreted and intracellular levels of α1-antitrypsin-mCherry were determined by quantification of fluorescence, as previously described. As shown in Supplemental Figure 4A, the amount of secreted α1-antitrypsin in HeLa cells transfected with pSERPINA1[Z]-mCherry was reduced to 50% of the amount secreted from cells transfected with pSERPINA1[M]-mCherry. The reduction in α1-antitrypsin secretion correlated with an increase in the intracellular level of α1-antitrypsin in cells transfected with pSERPINA1[Z]-mCherry compared with cells transfected with pSERPINA1[M]-mCherry (Supplemental Figure 4B). To evaluate whether reduced secretion and increased intracellular levels of the Z variant in this setup were due to accumulation of α1-antitrypsin in the ER, as previously demonstrated (19), transfected HeLa cells were stained for the ER using an antibody recognizing KDEL (Supplemental Figure 4C). Notably, in cells transfected with pSERPINA1[M]-mCherry, α1-antitrypsin-mCherry colocalized with ER in a reticular-like structure. However, in contrast, in cells transfected with pSERPINA1[Z]-mCherry, foci were formed and retained in ER, exactly as we observed for accumulating C1INH, resulting in structural changes of the ER.

In summary, these data consolidate the use of this cell model system for studies of serpin localization and secretion. Our findings suggest that the cellular aggregation phenotypes induced by the α1-antitrypsin Z variant and $C1INH_{Gly162\_Pro206del}$ encoded by SERPING1[c.551_685del] share important characteristics and lend support to the notion that serpin aggregation affects C1INH secretion in patients with the c.551_685del mutation, similar to how the Z mutation affects secretion of α1-antitrypsin in A1ATD patients.

Colocalization of normal and defective C1INH protein in focus-forming aggregates. To determine if normal and defective C1INH protein colocalize within the formed protein foci, HeLa cells

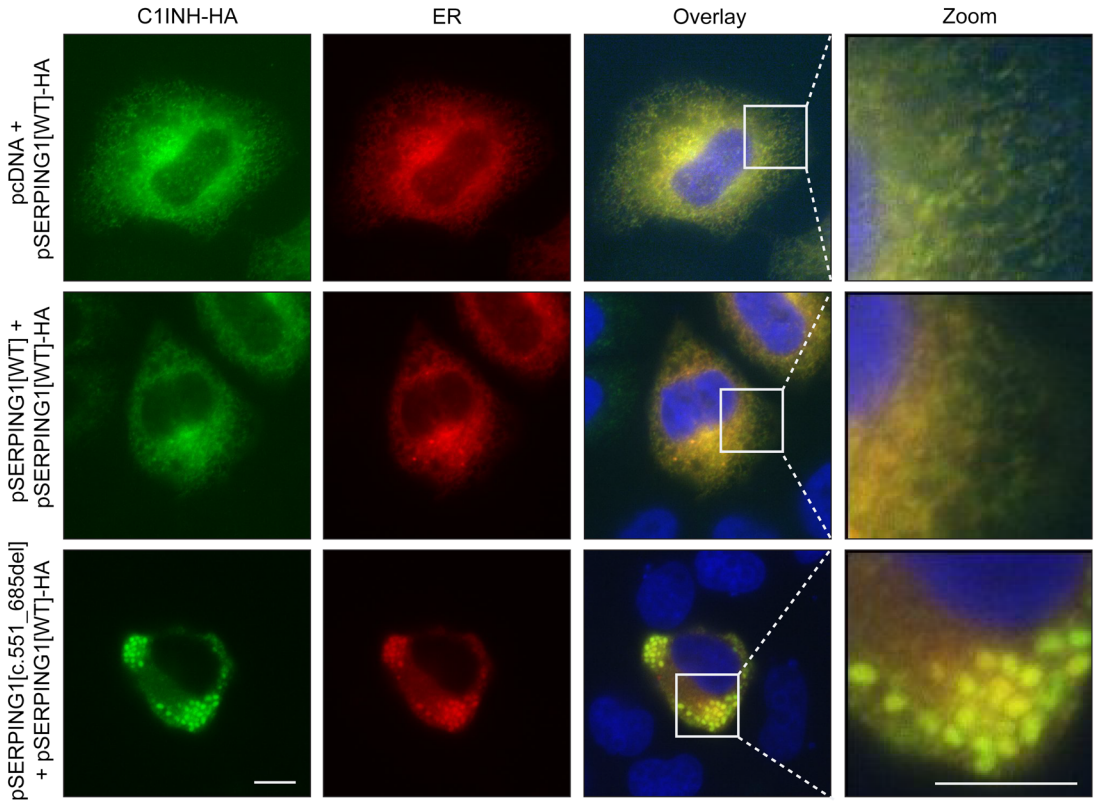

Figure 5. Intracellular retention of C1INH in the ER. HeLa cells were cotransfected with pSERPING1[WT]-HA and pcDNA, pSERPING1[WT], or pSERPING1[c.551_685del]. To visualize ER, an expression plasmid encoding the Tomato fluorescence gene fused to an endoplasmic reticulum–targeting sequence was included in the transfections (red). At 48 hours after the cotransfections, the cells were fixated and incubated with a HA-antibody and Hoechst to visualize normal C1INH-HA (green) and the nuclei (blue), respectively. Scale bars: 10 μm. Data are representative of findings from more than 3 biological replicates, and similar results were seen in at least 3 independent experiments.

were cotransfected with pSERPING1[WT]-mCherry and pSERPING1[c.551_685del]-HA, producing differently tagged C1INH variants, which allowed us to distinguish between normal and defective C1INH protein. Cells cotransfected with pSERPING1[WT]-mCherry and pSERPING1[WT]-HA were included as a control. As expected, C1INH foci were only formed in cells in which pSERPING1[WT]-mCherry was cotransfected with pSERPING1[c.551_685del]-HA, and normal C1INH-mCherry and C1INH$_{Gly162_Pro206del}$-HA protein localized to the same cellular structures (Figure 6A). In summary, these data support that physical colocalization of mutant and normal C1INH contributes to aggregate formation and the dominant-negative effects of defective C1INH protein.

Normal C1INH and C1INH$_{Gly162_Pro206del}$ are directly associated in C1INH polymers. To investigate whether formation of aggregates consisting of normal C1INH and C1INH$_{Gly162_Pro206del}$ involved direct association between the 2 variants, we performed coimmunoprecipitation (co-IP) assays using different sets of tagged variants. First, untagged normal and C1INH$_{Gly162_Pro206del}$ were separately expressed or coexpressed in HeLa cells. Using a C1INH antibody detecting both C1INH protein variants, we first verified by Western blotting that secretion of C1INH$_{Gly162_Pro206del}$ was markedly reduced relative to normal C1INH (Figure 6B, top panel; Supplemental Figure 5A). Notably, as opposed to cells expressing normal C1INH, higher amounts of C1INH protein were detected in the soluble and insoluble fractions of cellular protein derived from cells expressing the disease variant (Figure 6B, bottom panels; Supplemental Figure 5, B and C). These findings recapitulated that aggregated C1INH protein accumulated in cells expressing C1INH$_{Gly162_Pro206del}$. Next, we coexpressed HA-tagged normal C1INH with C1INH$_{Gly162_Pro206del}$ in HeLa cells and noted the inhibitory effect of C1INH$_{Gly162_Pro206del}$ on secretion of HA-tagged C1INH relative to cells expressing normal C1INH-HA alone (Figure 6C, top panel; Supplemental Figure 5D). Interestingly, only in the presence of C1INH$_{Gly162_Pro206del}$, HA-tagged normal C1INH also appeared in the insoluble fraction of cellular protein, suggesting that normal protein was restrained in the insoluble fraction by the mutated protein (Figure 6C, lower panels; Supplemental Figure 5, E and F). Finally, we transfected HeLa cells with plasmid encoding either V5-tagged normal C1INH or HA-tagged C1INH$_{Gly162_Pro206del}$, or cotransfected with a combination of these variants, and performed co-IP on whole-cell lysates by incubating with anti–V5-coupled beads to capture V5-tagged protein and potential interacting proteins. It was verified first that V5- and HA-tagged C1INH variants were equally present in the input (Figure 6D, top panel; Supplemental Figure 5, G and H). As the presence of C1INH-V5 was evident in the captured fraction, we then blotted for the presence of HA-tagged C1INH protein among captured complexes. Notably, HA-tagged C1INH$_{Gly162_Pro206del}$ was detected when the protein was expressed together with V5-tagged C1INH, whereas normal HA-tagged protein was not captured in the presence of V5-tagged

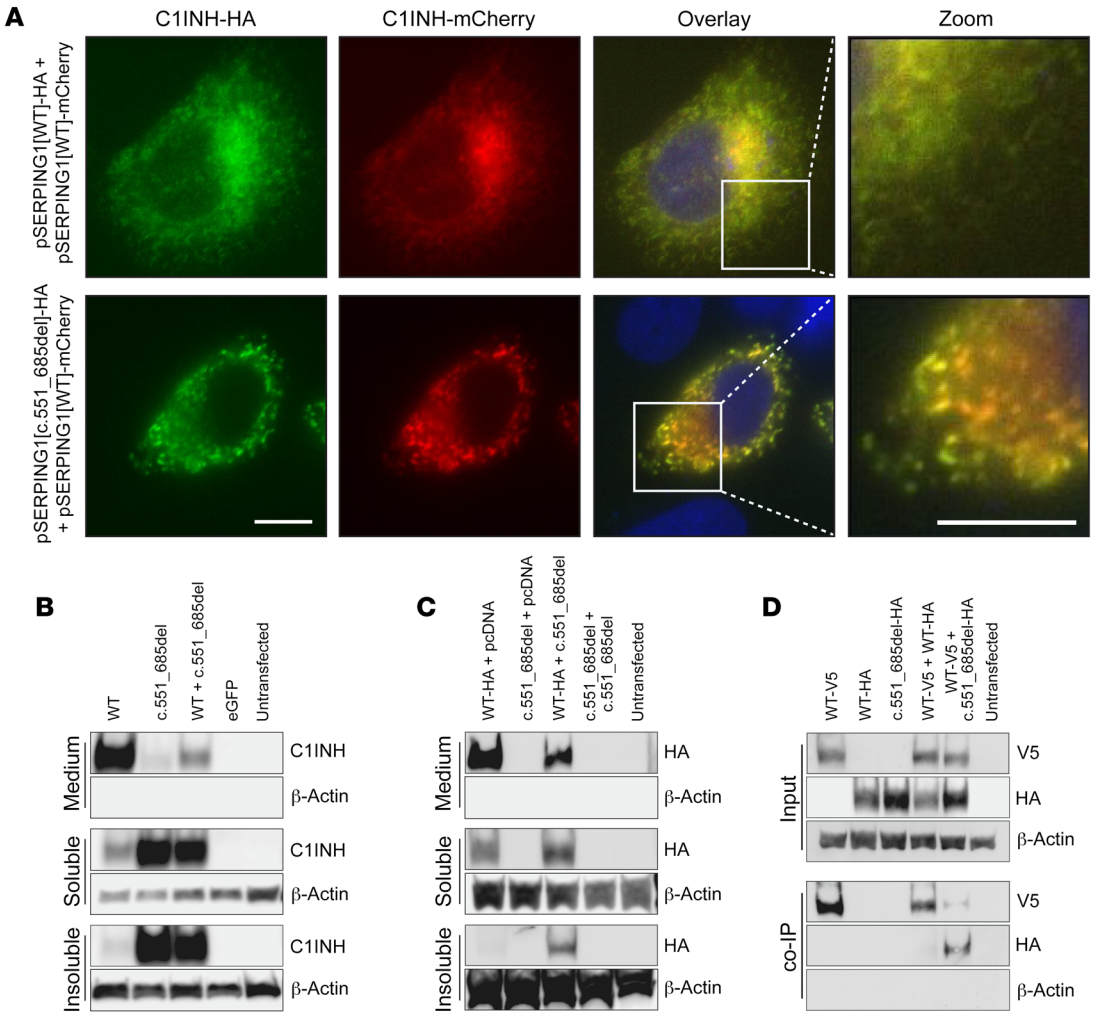

Figure 6. Direct interaction between normal C1INH and C1INH$_{Gly162_Pro206del}$. (**A**) Colocalization of normal and mutated C1INH. Widefield microscopy of HeLa cells cultured for 48 hours after cotransfection with SERPING1[WT]-mCherry and SERPING1[WT]-HA or SERPING1[c.551_685del]-HA. C1INH-HA was visualized with HA-specific antibody (green) and nuclei with Hoechst (blue). Scale bars: 10 μm. (**B** and **C**) Western blot analysis of total protein in medium as well as soluble and insoluble protein fractions derived from HeLa cells cultured for 72 hours after transfection or cotransfection with 900 ng plasmid DNA in total. Separation of soluble and insoluble C1INH fractions by centrifugation of whole cell lysate at 12,000*g* for 20 minutes at 4°C. (**B**) Detection of C1INH$_{Gly162_Pro206del}$ in the insoluble fraction. HeLa cells were transfected with 900 ng pSERPING1[WT] or pSERPING1[c.551_685del] or cotransfected with 450 ng pSERPING1[WT] and 450 ng pSERPING1[c.551_685de]. C1INH levels were detected using PAb C1INH antibody. (**C**) Normal C1INH in the insoluble fraction induced by C1INH$_{Gly162_Pro206del}$. HeLa cells were cotransfected with 450 ng pSERPING1[WT]-HA and either 450 ng pcDNA or pSERPING1[c.551_685del]. Normal C1INH-HA levels were detected with HA-specific antibody. (**D**) Direct protein-protein interaction between normal and mutated C1INH. Coimmunoprecipitation on whole cell lysate from HeLa cells cultured for 48 hours after transfection or cotransfection with 40 μg plasmid DNA in total. HeLa cells were transfected with pSERPING1[WT]-V5, pSERPING1[WT]-HA, or pSERPING1[c.551_685del]-HA, or cotransfected with pSERPING1[WT]-V5 and pSERPING1[WT]-HA or pSERPING1[c.551_685del]-HA. A small amount of the whole cell lysate was saved (input) and the remaining lysate incubated with anti-V5 coupled beads to capture normal V5-tagged C1INH and interacting proteins (co-IP). Presence of normal C1INH-V5 and C1INH[Variant]-HA was visualized with V5- and HA-specific antibodies as relevant. (**A**) Data are representative of findings from more than 3 biological replicates. (**A**–**C**) Similar results were seen in at least 2 independent experiments. (**B**–**D**) Transfections were carried out in triplicate (n = 3).

C1INH (Figure 6D, lower panel; Supplemental Figure 5, I and J). These findings demonstrate that direct protein-protein interactions are formed between normal C1INH and the HAE-causing C1INH$_{Gly162_Pro206del}$ variant, whereas normal C1INH does not alone engage in such complex formation.

C1INH aggregates are prominent in patient fibroblasts carrying the c.551_685del SERPING1 gene variant. To our knowledge, aggregates of C1INH protein have not previously been detected in cells derived from HAE type I patients. It was critical, therefore, to investigate whether aggregate formation was also evident in C1INH-expressing patient cells. As we did not have access to patient hepatocytes, we set out to study C1INH production and secretion in cultures of skin-derived fibroblasts, as was previously demonstrated by Kramer and colleagues (31). Fibroblasts were isolated and expanded from 3 HAE type I patients carrying the c.550G>A, c.551_685del, and c.838_846del *SERPING1* alleles, respectively. First, to confirm that patient-derived fibroblasts could be exploited as a cellular model of the disease, C1INH secretion from each of the cultures as well as from 3 fibroblast cultures derived from healthy donors was measured by sandwich ELISA.

Notably, for all 3 patients, secretion of C1INH from fibroblasts was significantly reduced relative to the controls (Figure 7A). For 2 of the 3 patient samples (c.551_685del and c.838_846del), secretion was severely reduced, resulting in C1INH medium levels corresponding to 10%–30% of the levels observed with the controls (Figure 7A). Among the 6 samples, some variation in the levels of *SERPING1* mRNA was observed. Despite a vague indication of lower mRNA levels in patient samples, comparable levels of *SERPING1* mRNA were measured in patient-derived cells relative to the control showing the lowest level of expression (NHDF-15) (Figure 7B), suggesting that differences in C1INH secretion did not reflect major differences in RNA production or processing. Notably, using fibroblasts derived from the patient carrying the c.551_685del allele, we performed a PCR on cDNA with *SERPING1* primers spanning the deletion and demonstrated by gel analysis that the normal allele and the allele carrying the deletion were equally expressed in the patient cells (Figure 7B, inset).

To demonstrate the impact of the c.838_846del allele on the normal allele, we first transduced primary fibroblasts (NHDF-03) from a homozygous healthy donor with lentiviral vectors encoding c.551_685del at an estimated MOI of 1. Relative to untransduced cells and cells treated with eGFP-encoding lentiviral vectors, secretion from cells expressing the mutant protein was severely restricted, resulting in levels that were almost halved compared with the controls (Figure 7C). Collectively, these findings were consistent with a model by which C1INH encoded by the disease allele induced reduced secretion by dominant-negative actions.

To investigate whether aggregate formation and structural ER changes were evident in fibroblasts from the patient carrying the c.551_685del allele, we transfected control and patient-derived fibroblasts with the expression plasmid encoding the Tomato fluorescence gene fused to an ER-targeting sequence. In all 3 cultures of control fibroblasts (derived from 3 different donors) a diffuse and reticular-like ER structure corresponding to the structure that was observed in HeLa cells expressing only normal C1INH (Figure 5) was observed (Figure 7D). Importantly, in fibroblasts derived from the patient, we noted that the overall ER structure was significantly different (Figure 7D, right panel) and very similar to the ER structure that we observed in HeLa cells cotransfected with pSERPING1[WT]-mCherry and pSERPING1[c.551_685del] (Figure 5).

Next, we transfected control and patient-derived fibroblasts with plasmid encoding the ER-targeted Tomato fluorescence protein and then stained the cells with a monoclonal C1INH antibody recognizing both normal and defective C1INH protein. In all control fibroblasts, C1INH colocalized with the reticular-like ER structure (Figure 7E), as seen earlier in the transfected control samples of HeLa cells. In patient cells, in contrast, the staining of C1INH revealed a distinct, speckled pattern that was significantly different from the pattern in control fibroblasts, demonstrating that C1INH and fluorescent ER-targeted protein localized to the same cellular structures (Figure 7E). We confirmed this cellular phenotype by staining fibroblasts that were cotransfected with pSERPING1[WT]-HA and plasmid encoding the Tomato fluorescence gene fused to an ER-targeting sequence with an HA-specific antibody (Supplemental Figure 6). In conclusion, our data unveil aberrant accumulation of C1INH protein and the appearance of a distinct ER structural phenotype in cells from a HAE type I patient carrying a heterozygous in-frame deletion within the *SERPING1* gene.

Identification of other dominant-negative HAE-causing SERPING1 variants. Aggregate formation caused by protein-protein interactions between normal and mutated C1INH explains a dominant-negative phenotype resulting in reduced secretion of functional C1INH. However, among the HAE-causing mutations that were initially selected for this study, the severity of aggregate formation varied, and larger protein aggregation foci formed in the presence of both normal and mutant protein were seen only for 2 variants (c.551_685del and c.566C>A). Considering the wealth of different *SERPING1* variants causing HAE, we set out to identify other *SERPING1* alleles acting through similar mechanisms. Since the shutter domain of the protein is afflicted in C1INH derived from both the c.551_685del and c.566C>A variants, we decided to focus on this region of the protein and identified the β-sheets and α-helices that are part of or in close proximity to the shutter domain. A total of 10 HAE-causing *SERPING1* variants were selected from the C1 inhibitor gene mutation database (32). Each of these 10 gene variants encodes a full-length C1INH protein (478-aa) with a single amino acid change within or near the shutter domain (Figure 8A; Supplemental Figure 7 and Supplemental Table 2). First, by transfection of expression constructs (pSERPING1[Variant]) into HepG2 cells and subsequent Western blot analysis, we observed robust protein production and reduced secretion of C1INH for 8 of the 10 variants, as measured 72 hours after transfection (Figure 8B; Supplemental Figure 8, A and B). For 3 of these variants, c.508T>C, c.530T>C, and c.707T>C, secretion was entirely blocked. Next, to investigate the inhibitory impact of mutated C1INH on normal C1INH, we cotransfected the expression constructs with the pSERPING1[WT]-mCherry reporter construct and measured mCherry intensity in medium and in cells. For 5 of the variants, we found that secretion of the mCherry-tagged normal C1INH was inhibited by the mutant protein, like the effect caused by the c.551_685del variant (Figure 8C). Also, for some of the variants we found that the intracellular levels of C1INH-mCherry were significantly increased although not with the same impact as reproducibly observed for the c.551_685del variant (Figure 8D). We demonstrated that these effects were evident already 48 hours after transfection (Supplemental Figure 9). Interestingly, by wide-field microscopy, we observed formation of foci containing normal mCherry-tagged C1INH in cells expressing the c.530T>C, c.707T>C, c.863_864TC>AA, and c.871A>C *SERPING1* variants (Figure 9A). Importantly, none of the 10 C1INH variants showed any indication of forming protein aggregates, when they were expressed separately (and in the absence of normal C1INH) in HeLa cells (Supplemental Figure 10). However, normal C1INH-HA was prevalent in the insoluble protein fraction derived from cells in which normal C1INH-HA was coexpressed with C1INH from the c.508T>C, c.530T>C, c.707T>C, c.863_864TC>AA, and c.871A>C gene variants (Figure 9B, lower panel; quantifications in Supplemental Figure 11, A–C). This mimicked the pattern that we also observed for c.551_685 del (included as control in Figure 9B). In contrast, for cells cotransfected with pSERPING1[WT]-HA and pcDNA, normal C1INH-HA was detectable in the soluble protein fraction, but not in the insoluble fraction (Figure 9B, middle and lower panel).

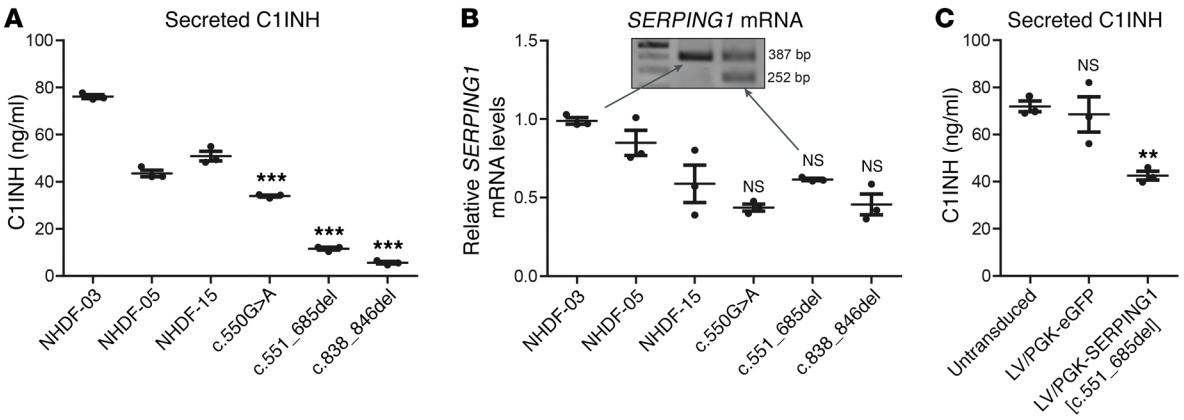

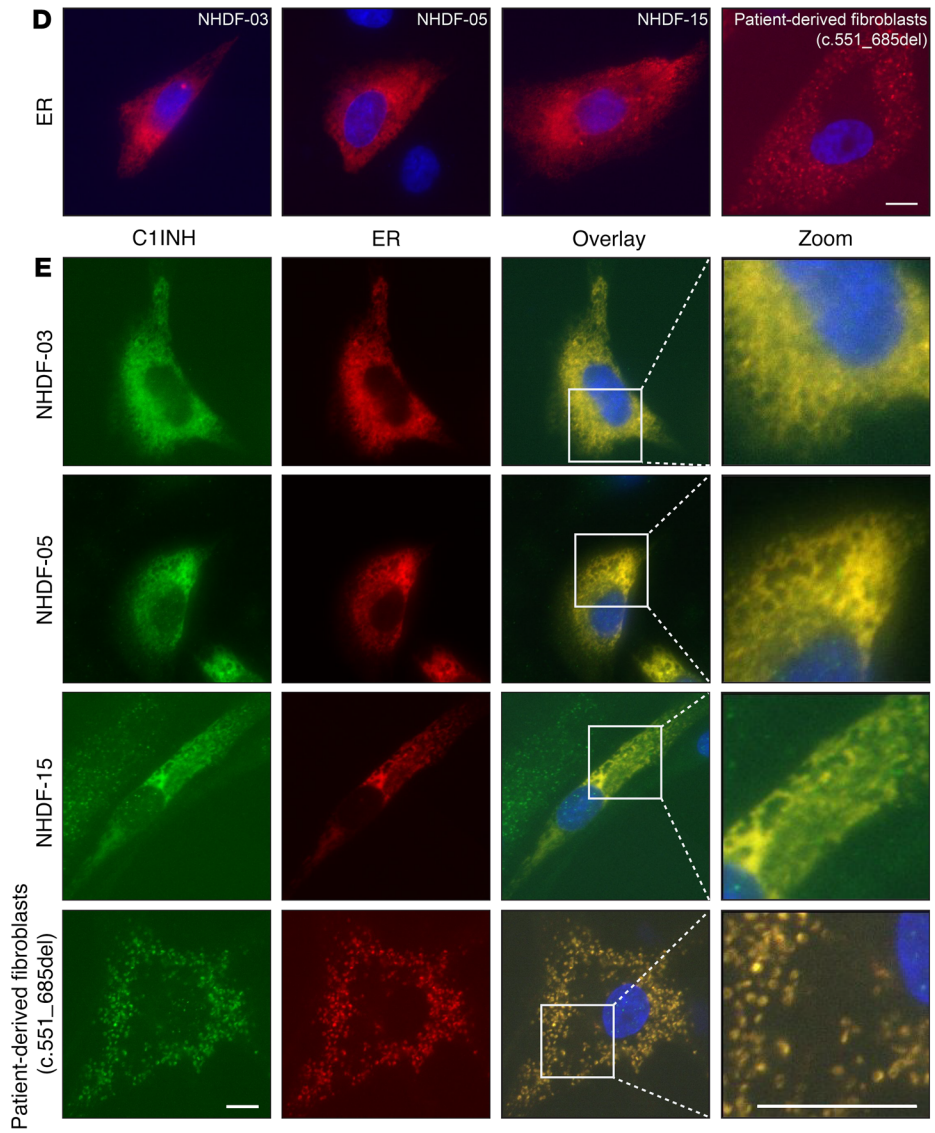

Figure 7. Correlation of reduced C1INH secretion in skin-derived fibroblasts derived from a patient carrying the c.551_685del mutation with C1INH accumulation in ER. (**A**) C1INH in medium from control (NHDF-03, NHDF-05, NHDF-15) and patient-derived fibroblasts. (**B**) Evaluation of *SERPING1* mRNA expression levels in control and patient-derived fibroblasts by qPCR. Equal expression of normal and mutant *SERPING1* alleles in fibroblasts derived from the patient carrying the c.551_685del mutation. Inset: Agarose gel showing PCR products from PCR amplification (using primers spanning the deletion) on cDNA synthesized from RNA purified from either control NHDF-03 fibroblasts or patient-derived fibroblasts. (**C**) Restricted C1INH secretion induced by lentiviral delivery of *SERPING1*[c.551_685del]. Control NHDF-03 fibroblasts were transduced with lentiviral vectors encoding $C1INH_{Gly162\_Pro206del}$ (or eGFP as control) at an estimated MOI of 1. (**D**) Structure of the ER in control fibroblasts and fibroblasts derived from the c.551_685del patient. The fibroblasts were transfected with 900 ng plasmid encoding the Tomato fluorescence gene fused to an ER-targeting sequence to visualize ER (red). Cells were fixated 48 hours after transfections, and nuclei visualized with Hoechst (blue). Scale bar: 10 μm. (**E**) Accumulation of endogenous C1INH within the ER of patient-derived fibroblasts. The fibroblasts were transfected as in **D**, fixated, and incubated with Hoechst to visualize the nuclei (blue) and C1INH antibody to visualize both normal and mutated C1INH (green). Scale bars: 10 μm. (**A**–**C**) The experiment was carried out in triplicate ($n = 3$), and data are mean ± SEM. $^{*}P < 0.05$, $^{**}P < 0.01$, $^{***}P < 0.001$, patient-derived fibroblasts compared with NHDF-05 (**A**) or NHDF-15 (**B**) or transduced compared with untransduced NHDF-03 (**C**). Statistical analyses were performed by 1-way ANOVA with Dunnett's multiple comparison test. (**D**–**E**) Data are representative of findings from more than 3 biological replicates. (**A**–**E**) Similar results were seen in at least 2 independent experiments.

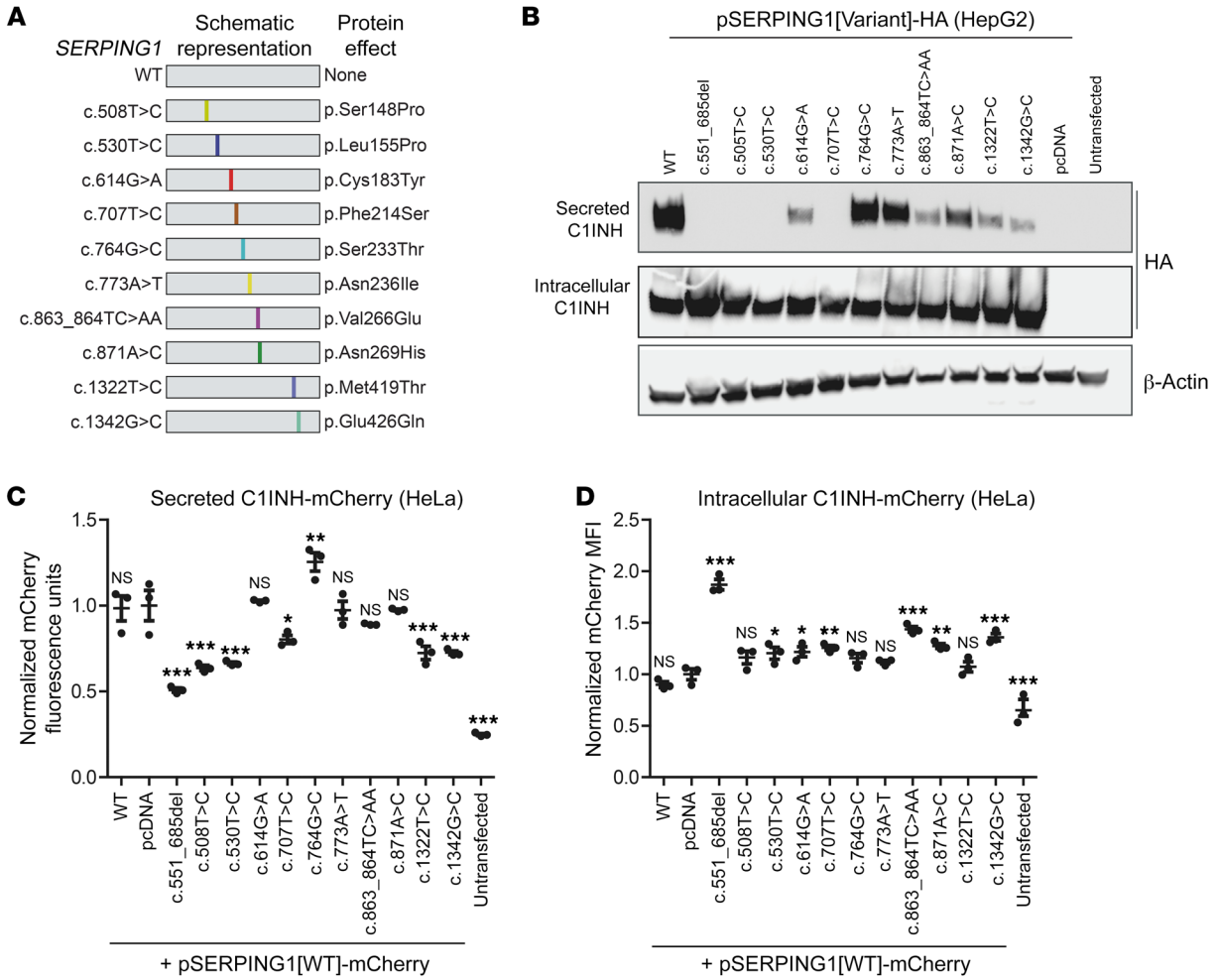

Figure 8. Dominant-negative properties of additional HAE-causing *SERPING1* gene variants. (**A**) Schematic representation of studied *SERPING1* gene variants. See Supplemental Table 2 for additional information. (**B**) Western blot analysis of medium and total protein derived from HepG2 cells transfected with 900 ng pSERPING1[Variant]-HA. The C1INH-HA levels were detected using a HA-specific antibody. (**C** and **D**) Secretion and intracellular levels of normal C1INH-mCherry in HeLa cells cotransfected with 450 ng pSERPING1[WT]-mCherry and 450 ng pSERPING1[Variant]. (**B**–**D**) Transfections were carried out in triplicate ($n = 3$), and similar results were seen in at least 2 independent experiments. (**C** and **D**) $^{*}P < 0.05$, $^{**}P < 0.01$, $^{***}P < 0.001$, compared with pcDNA. Statistical analyses were performed by 1-way ANOVA with Dunnett's multiple comparison test.

Finally, for the 3 variants (c.530T>C, c.707T>C, and c.863_864TC>AA) showing both reduced secretion and dominant-negative intracellular retention of normal C1INH as well as the capacity to induce aggregation of normal C1INH, we performed Co-IP to unveil protein-protein interactions between C1INH variants and normal C1INH. Again, HA-tagged disease variants were coexpressed with V5-tagged normal protein and capture of V5-tagged C1INH was verified by Western blotting (Figure 9C; quantifications in Supplemental Figure 11, D–G). Notably, by blotting among captured protein complexes using an HA-specific antibody, we detected considerable amounts of HA-tagged C1INH protein, demonstrating that all 3 disease-causing C1INH variants engaged in direct protein-protein interactions with normal C1INH (Figure 9C, lower panel). Collectively, these findings suggest that dominant-negative phenotypes involving protein-protein association and aggregate formation are evident for several *SERPING1* variants causing HAE.

Amelioration of reduced C1INH secretion in HAE type I patient fibroblasts by delivery of a therapeutic SERPING1 gene. The identification of a dominant-negative disease mechanism leading to HAE type I may inspire new ways to restore C1INH secretion and treat HAE type I. Here, we focus on exploiting genetic strategies to overcome restriction on C1INH secretion caused by C1INH protein aggregation induced by the dominant-negative effect of mutant C1INH protein. To study whether such inhibitory effects could be overcome by delivering a gene expression cassette coding for normal C1INH, we initially created HeLa cells carrying expression cassettes encoding either normal C1INH or $C1INH_{Gly162\_Pro206del}$ (from SERPING1[c.551_685del]). Next, we transduced these cell lines with lentiviral vectors carrying the SERPING1[WT] cDNA expressed from the phosphoglycerate kinase (PGK) promoter. Untransduced cells as well as cells transduced with eGFP-encoding lentiviral vectors were included as controls. As expected, secretion of C1INH was dramatically higher from untransduced cells expressing the WT *SERPING1* gene compared with cells expressing $C1INH_{Gly162\_Pro206del}$ (Figure 10A). In addition, treatment of C1INH-secreting HeLa cells with

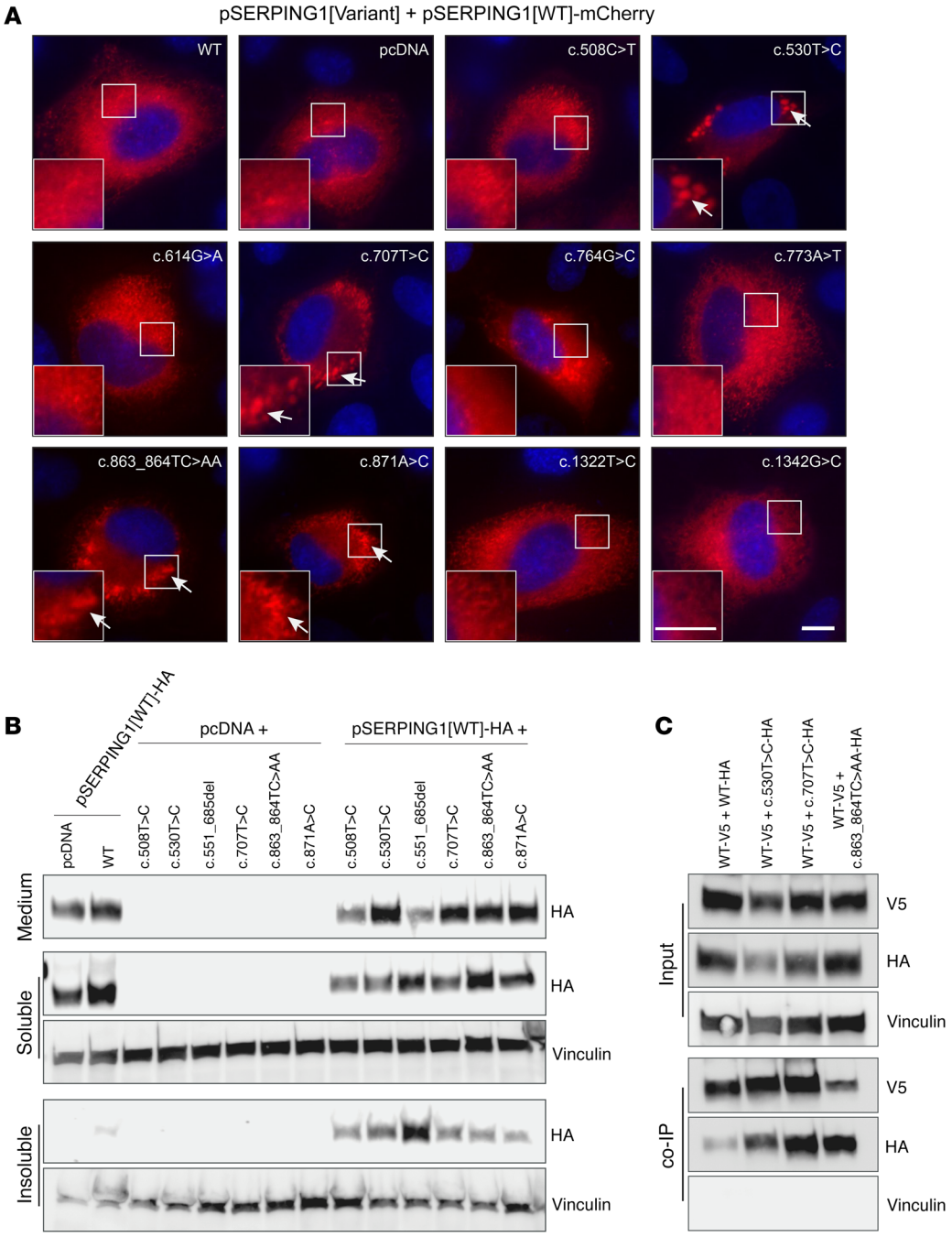

Figure 9. Formation of C1INH aggregates containing associated normal and mutant C1INH induced by dominant-negative *SERPING1* gene variants causing HAE. (**A**) Live widefield microscopy of HeLa cells cultured for 48 hours after cotransfection with 450 ng pSERPING1[WT]-mCherry and 450 ng pSERPING1[Variant]. Aggregates are indicated with arrows. Scale bars: 10 μm. (**B**) Western blot analysis of medium, soluble and insoluble C1INH derived from HeLa cells cultured for 72 hours after cotransfection with 450 ng pSERPING1[WT]-HA and 450 ng pSERPING1[Variant]. The experiment was carried out as described in Figure 6, B and C. (**C**) Coimmunoprecipitation on cell lysate from HeLa cells cultured for 48 hours after cotransfection with 20 μg pSERPING1[WT]-V5 and 20 μg pSERPING1[Variant]-HA. The experiment was carried out as described in Figure 6D. (**A** and **B**) Data are representative of findings from more than 3 biological replicates and similar results were seen in at least 2 independent experiments. Transfections were carried out in triplicate (n = 3; **B**) or duplicate (n = 2; **C**).

C1INH-encoding lentiviral vectors increased the level of secreted C1INH from 1,000 to 4,500 ng/ml, whereas treatment with the viral vector raised the level of secreted C1INH from cells expressing $C1INH_{Gly162\_Pro206del}$ from background level to 2,500 ng/ml (Figure 10A). These findings indicated that the restrictive effect of the mutant variant could be overcome by viral gene transfer. To test this gene therapy delivery approach directly in patient cells, we delivered C1INH-expressing lentiviral vectors and control vectors to control and patient fibroblasts. For all control fibroblasts, we observed a marked increase in the secretion of C1INH, leading to levels in the medium ranging from 7,000 to 12,000 ng/ml (Figure 10B). Also in these cells, we observed a tendency to reduced C1INH secretion upon treatment with eGFP-encoding lentiviral vectors (although not with statistical significance), potentially indicating a toxic or inhibitory effect of eGFP. Most importantly, we found that secretion of C1INH from fibroblasts carrying the c.551_685del allele was robustly increased, although to a lesser extent than in control fibroblasts, after lentiviral *SERPING1* gene delivery boosting the level of C1INH in the medium to 4,000 ng/ml (Figure 10B). Thus, the dominant-negative effects of the disease allele seemed to lower the total protein output in patient cells, but did not severely restrict secretion of ectopically expressed C1INH protein. These findings support the notion that conventional gene addition therapy approaches can treat the disease and can be developed for future treatment also of HAE type I involving dominant-negative disease mechanisms.

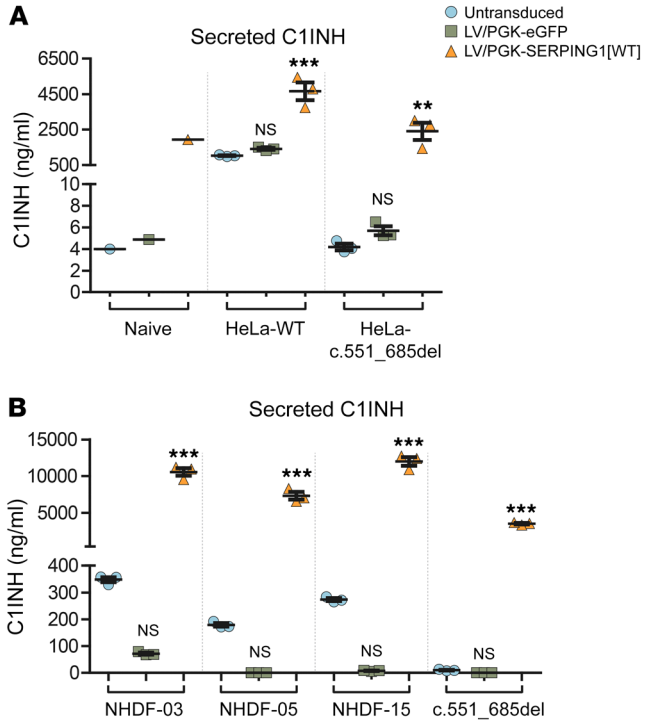

Figure 10. Increased C1INH secretion after lentiviral delivery of WT *SERPING1* gene models HAE gene therapy in fibroblasts from patients carrying a dominant-negative disease allele (*SERPING1*[c.551_685del]). (**A**) HeLa-WT and HeLa-c.551_685del cell populations (3 of each) were created by transduction of naive HeLa cells with lentiviral vectors encoding normal C1INH or $C1INH_{Gly162\_Pro206del}$. Stably transduced and naive HeLa cells were reseeded and transduced with lentiviral vectors encoding eGFP or normal C1INH. Transduction of each of the 3 cell populations was carried out in triplicate ($n = 3$) and the medium was pooled for each transduced cell population prior to C1INH measurements. For the naive cell line, cells were transduced and medium pooled prior to C1INH measurement, resulting in only a single data point for each treatment. (**B**) Control and patient-derived fibroblasts were transduced with lentiviral vectors encoding normal C1INH or eGFP as a control. Transductions were carried out in triplicate ($n = 3$). (**A** and **B**) Data are mean ± SEM. $^{**}P < 0.01$, $^{***}P < 0.001$, compared with untransduced cells in each group. NS indicates lack of statistical significance between untransduced and LV/PGK-eGFP–treated groups. Statistical analyses were performed by 1-way ANOVA with Dunnett's multiple comparison test. (**B**) Similar results were seen in at least 2 independent experiments. LV, lentiviral vectors.

Discussion

Since the initial description of HAE by Osler in 1888 (33), and later fundamental studies by Donaldson linking HAE with C1INH deficiency (34), the growing understanding of the disease pathophysiology of HAE has resulted in different HAE treatment modalities, including intravenous C1INH concentrates and subcutaneous bradykinin receptor antagonists. However, cellular disease mechanisms responsible for the reduced levels of functional C1INH in the blood of HAE type I patients, compared with healthy individuals, are yet to be elucidated. A better understanding of the cellular pathology of HAE type I is essential to improve individualized treatment and pave the way for new effective treatments of the disease including genetic therapies. Based on earlier studies, it has been suggested that defective C1INH causes HAE type I through vaguely described trans-inhibitory actions that may cause reduced functional C1INH plasma levels in HAE type I patients by negatively affecting synthesis, intracellular transport, or secretion of normal C1INH protein (29, 35). Speculations suggesting that C1INH variants that are defective in intracellular transport may negatively affect transport of normal C1INH were laid out 25 years ago (36). However, such trans-inhibitory mechanisms still remain to be unraveled.

In this study, we report that defective C1INH protein, at least for a subset of HAE type I patients, has the capacity to reduce the secretion of normal C1INH protein in a dominant-negative fashion. Restricted secretion correlates with intracellular accumulation of both defective and normal C1INH protein in the ER and the formation of aggregates consisting of both C1INH variants linked by protein-protein interactions. We specifically studied skin-derived fibroblasts from a HAE type I patient carrying a dominant-negative allele with a severe cellular phenotype and confirmed that C1INH protein retention caused by aggregation was evident in patient cells. In this patient-derived cellular model system, we also showed that increased levels of C1INH secretion could be achieved by delivery of the WT *SERPING1* gene, demonstrating benefits of genetic restoration despite the dominant-negative effects of the disease gene. Additionally, we found that secretion of normal C1INH from fibroblasts derived from healthy donors is restricted when a dominant-negative allele is transferred to the cells using a lentiviral delivery approach.

Protein polymer formation is a characteristic of serpinopathies like A1ATD and FENIB. In both cases, polymers of mutated serpins have been shown to accumulate within the ER (19, 20, 22). Miranda and colleagues established a cellular model of FENIB that reproduced aggregation of mutated neuroserpin polymers in the ER, as seen in the patients, and found that the accumulation of neuroserpin within the ER was associated with a structural change of the ER (37). Similarly, in our study, aggregates of C1INH protein were found to accumulate within the ER in both HeLa cells cotransfected with plasmids encoding normal and defective C1INH variants and in fibroblasts from a Danish type I HAE patient carrying the c.551_685del *SERPING1* gene variant. Detection of C1INH aggregates in the ER correlates with previous findings, in which mutant C1INH was found to be sensitive to endoglycosidase H (endoH) (35, 36). Furthermore, the accumulation within the ER was reflected by structural change of the ER, suggesting that C1INH protein retention potentially affects ER function in C1INH-expressing cells in patients and has a wider impact on cellular homeostasis.

Biochemical analysis of neuroserpin polymers, isolated from the brain of a patient with FENIB, revealed that neuroserpin polymers were composed of mutant neuroserpin only (38). Along these lines, the polymerization rates of normal and defective α1-antitrypsin are not affected by the mixing of normal and defective protein (39), suggesting that the disease-causing protein

in A1ATD is not directly affecting the normal protein. This is in accordance with the recessive inheritance of A1ATD. In contrast to these findings, we found that 7 of 16 analyzed HAE-causing C1INH variants (encoded by SERPING1[c.551_685del], SERPING1[c.550G>A], SERPING1[c.566C>A], SERPING1[c.530T>C], SERPING1[c.707T>C], SERPING1[c.863_864TC>AA], and SERPING1[c.871A>C]) caused formation of aggregates containing normal C1INH. Additionally, normal and defective C1INH protein was found to colocalize in such aggregates, and Co-IP assays stated for all relevant C1INH variants that formation of aggregates involves direct protein-protein interaction between normal and mutated C1INH protein. Interestingly, except for cells expressing $C1INH_{Thr167Asn}$ (encoded by SERPING1[c.566C>A]), we did not observe aggregate formation for any of the studied C1INH variants, when the protein was expressed in the absence of normal C1INH. This indicates that C1INH aggregates are prone to be formed when both functional and defective C1INH proteins are present and involves unique lock-and-key interactions between normal C1INH and disease-causing variants, providing further support to the notion that defective C1INH reduces the secretion of normal C1INH by directly inducing its retention. $C1INH_{Thr167Asn}$ encoded by SERPING1[c.566C>A] appeared to represent a unique variant for which induced formation of polymers did not necessarily require normal C1INH, although the mutant protein did indeed influence accumulation of coexpressed normal C1INH. As the patient carrying this specific *SERPING1* variant showed C1INH blood levels that were only slightly reduced relative to healthy individuals, one may speculate that normal C1INH in this patient was to some degree left untouched as a result of the tendency of $C1INH_{Thr167Asn}$ to form homopolymers.

Throughout our studies, we observed the most severe cellular phenotypes triggered by $C1INH_{Gly162\_Pro206del}$ derived from the c.551_685del *SERPING1* gene variant due to the profound capacity of this variant to induce formation of C1INH aggregates in the presence of normal C1INH protein. In Danish patients expressing this exon 4–deleted mRNA, the disease allele contains a larger genomic deletion spanning exon 4 and including parts of the flanking introns. Notably however, splice site mutations in this region (typically in the splice acceptor site in the intron upstream of exon 4) can lead to formation of the exact same mutated protein, and HAE type I patients with this particular type of mutation have been described in previous reports (4, 40). Differences in the potential to form C1INH aggregates among the different HAE-causing C1INH variants and the particular severity of $C1INH_{Gly162\_Pro206del}$ may reflect how the mutation affects the structure of the C1INH protein. The c.551_685 deletion in the *SERPING1* gene leads to deletion of the whole exon 4, which induces significant structural changes in the C1INH protein, as exon 4 encodes both hD (Helix D), hC (Helix C), and s2A. Both hD and hC play an important role in stabilizing the shutter region (18), and deletion of these 2 helices may lead to opening of the sA, thereby allowing the RCL of other C1INH proteins to dock-in to the protein, allowing stable protein-protein interactions. Opening of the shutter domain may explain why aggregates are formed in cells coexpressing normal C1INH and $C1INH_{Gly162\_Pro206del}$ or some of the other variants causing aggregation and retention of C1INH. Interestingly, the c.530T>C, c.707T>C, and c.863_863TC>AA *SERPING1* gene variants (resulting in amino acid substitutions in hB, hE, and s3A, respectively, in C1INH protein), are all in very close proximity to the shutter domain and the region that is deleted in $C1INH_{Gly162\_Pro206del}$ (including hD, hC, and s2A) (see Supplemental Figure 12 for structural overview of the C1INH variations). Furthermore, deletion of exon 4 or other variations in the part of the protein encoded by this region may possibly lead to a less protruding RCL, potentially preventing it from aggregating with itself. This could explain why aggregate formation is predominant in the heterozygous situation where the mutant protein, like $C1INH_{Gly162\_Pro206del}$, is expressed simultaneously with normal C1INH.

Our discoveries suggest that HAE type I can be classified as a true serpinopathy with potential variations in cellular disease mechanisms depending on the specific *SERPING1* gene variant. Differences in the level of aggregate formation induced by the studied C1INH variants could potentially reflect that assays based on transient transfection in some cases do not allow sufficient time for the build-up of aggregates. At this stage, we cannot exclude that aggregate formation is part of the pathogenesis also for C1INH variants that did not in our hands induce a distinct cellular phenotype with formation of aggregates. Importantly, it cannot be ruled out that some of these variants cause disease through other trans-inhibitory mechanisms or that haploinsufficiency, potentially due to unbalanced gene expression from the 2 *SERPING1* alleles, results in development of the disease. Common for the far majority of the studied C1INH variants is that protein secretion, and not expression, is severely affected by the mutation, and in some patients this may potentially trigger haploinsufficiency even without the formation of aggregates. It should be noted that in our studies we excluded *SERPING1* variants giving rise to severely truncated C1INH variants or RNA degradation by nonsense-mediated decay. Therefore, disease-causing mechanisms for these variants still need to be described. More studies including a larger number of *SERPING1* variants will be essential to classify patients and their mutated gene variant according to the cellular disease mechanisms, including the dominant-negative mechanisms that we have unveiled here.

Like C1INH, α1-antitrypsin is primarily produced in the liver. Polymerization and intracellular retention of the mutated Z α1-antitrypsin variant within the ER of hepatocytes causes juvenile hepatitis, cirrhosis, and hepatocellular carcinoma (39). In our cellular model system, we found that the exact same cellular phenotype with massive aggregate formation appeared in cells expressing the Z α1-antitrypsin variant and in cells coexpressing normal and defective C1INH. Inevitably, this could indicate that liver damage observed in A1ATD patients could occur also in HAE type I patients. However, to our knowledge, liver damage has not in general been reported in HAE type I patients, indicating that such aggregate formation does not disturb normal liver function. Potential differences in aggregate formation could be explained by different levels of expression leading to differing intracellular concentrations of C1INH and A1AT, but potential explanations are currently speculative. In addition, although we observed severe aggregate formation in skin-derived fibroblasts, we did not have access to patient-derived hepatocytes, and cannot exclude that this particular cellular phenotype is less pronounced in the human liver. It is not unlikely that dominant-negative retention of normal C1INH may add to the consequences of haploinsufficiency, complicating the interpre-

tation of the cellular pathology, but this will have to be addressed in future studies, potentially in hepatocyte-like cells derived from patient-derived induced pluripotent stem cells (41, 42).

To the great benefit of patients, HAE type I is currently treated successfully with intravenously administered C1INH concentrates. However, as clinical gene therapy treatments of severe inherited conditions such as blindness (43), primary immunodeficiency (44), and hemophilia (45) are continuously showing great promise worldwide, it is not unrealistic to envision future genetic treatments also of HAE. Recently, work by Qiu and colleagues demonstrated reduced vascular leakage in skin and internal organs in a HAE mouse model treated intravenously with adeno-associated virus–based (AAV-based) vectors encoding functional C1INH (46). As HAE shares several similarities with hemophilia, invaluable experience from ongoing hemophilia B trials based on AAV-based gene delivery may eventually benefit HAE patients. Our discovery that HAE type I, at least in some patients, involves dominant-negative disease mechanisms, would argue that these patients would not be suitable for conventional gene therapy based on *SERPING1* gene transfer. Nevertheless, our studies in patient cells suggest that the dominant-negative effects of the disease allele can be overcome by viral vector-based gene delivery facilitating solid C1INH expression after gene delivery. It remains unclear, however, whether compromised ER function may affect posttranslational modification and overall functionality of ectopically expressed C1INH. As transgenic HAE mouse models carrying dominant-negative disease alleles are not currently available, further experimental consolidation of gene therapy benefits awaits the development of a mouse model that mimics the genetics and disease of the patients. Also, such a model, for example carrying the *SERPING1* exon 4 deletion, will allow future studies aimed at describing and resolving C1INH protein aggregation in the liver of heterozygous carriers of the dominant-negative disease mutation.

Methods

Complete descriptions of methods and materials are provided in the Supplemental Methods available online.

Statistics. All numerical data are presented as the mean ± SEM. Statistical analyses were performed with 1-way ANOVA with multiple comparisons for analysis of 3 or more groups, whereas 2-tailed Student's *t* test was only used for comparison of fewer than 3 groups. In all cases, *P* less than 0.05 was considered significant.

Study approval. All subjects gave informed written consent to the skin biopsy. The study was conducted in accordance with the Helsinki II Declaration and approved by the Regional Scientific Ethics Committee for Southern Denmark (project ID S-20120116).

Author contributions

DH and JGM designed research studies. DH, LBR, IR, and KAS cloned the plasmids. DH, LBR, SSM, MKT, and ABB conducted experiments and acquired data. DH, LBR, SSM, ABB, LNN, and JGM analyzed data. IR and AB isolated skin biopsies and analyzed patient data. LNN and TJC helped preparing and imaging cells. YP and CK produced antibodies. TF provided assistance for experiments carried out at the fluorescence scanner and coimmunoprecipitation. LNN, TJC, TF, YP, and CK provided reagents. DH and JGM wrote the manuscript.

Acknowledgments

We would like to thank Lisbeth Dahl Schrøder and Christian Knudsen for technical assistance. Flow cytometry was performed at the FACS Core Facility, Aarhus University, Denmark. This work was made possible through support from the Lundbeck Foundation, CSL Behring, Fonden af 1870, Robert Wehnerts og Kirsten Wehnerts Fond, Aage Bangs Fond, the A.P. Møller Foundation for the Advancement of Medical Science (Fonden til Lægevidenskabens Fremme), and the Oda og Hans Svenningsens Fond. DH is enrolled in and funded by the Graduate School of Health, Aarhus University. The Nikon microscope was funded by the Carlsberg Foundation (to LNN).

Address correspondence to: Jacob Giehm Mikkelsen, Department of Biomedicine, Aarhus University, Wilhelm Meyers Allé 4, DK-8000 Aarhus C, Denmark. Phone: 4587167767; Email: giehm@biomed.au.dk.

1. Bernstein JA. HAE update: epidemiology and burden of disease. *Allergy Asthma Proc*. 2013;34(1):3–6.
2. Germenis AE, Speletas M. Genetics of hereditary angioedema revisited. *Clin Rev Allergy Immunol*. 2016;51(2):170–182.
3. Bygum A. Hereditary angio-oedema in Denmark: a nationwide survey. *Br J Dermatol*. 2009;161(5):1153–1158.
4. Colobran R, Lois S, de la Cruz X, Pujol-Borrell R, Hernández-González M, Guilarte M. Identification and characterization of a novel splice site mutation in the SERPING1 gene in a family with hereditary angioedema. *Clin Immunol*. 2014;150(2):143–148.
5. Zuraw BL, Christiansen SC. HAE pathophysiology and underlying mechanisms. *Clin Rev Allergy Immunol*. 2016;51(2):216–229.
6. Rosen FS, Pensky J, Donaldson V, Charache P. Hereditary angioneurotic edema: two genetic variants. *Science*. 1965;148(3672):957–958.
7. Dewald G, Bork K. Missense mutations in the coagulation factor XII (Hageman factor) gene in hereditary angioedema with normal C1 inhibitor. *Biochem Biophys Res Commun*. 2006;343(4):1286–1289.
8. Bork K, et al. Hereditary angioedema with a mutation in the plasminogen gene. *Allergy*. 2018;73(2):442–450.
9. Bafunno V, et al. Mutation of the angiopoietin-1 gene (ANGPT1) associates with a new type of hereditary angioedema. *J Allergy Clin Immunol*. 2018;141(3):1009–1017.
10. Irving JA, Pike RN, Lesk AM, Whisstock JC. Phylogeny of the serpin superfamily: implications of patterns of amino acid conservation for structure and function. *Genome Res*. 2000;10(12):1845–1864.
11. Gettins PG. Serpin structure, mechanism, and function. *Chem Rev*. 2002;102(12):4751–4804.
12. Heit C, et al. Update of the human and mouse SERPIN gene superfamily. *Hum Genomics*. 2013;7:22.
13. Law RH, et al. An overview of the serpin superfamily. *Genome Biol*. 2006;7(5):216.
14. Silverman GA, et al. The serpins are an expanding superfamily of structurally similar but functionally diverse proteins. Evolution, mechanism of inhibition, novel functions, and a revised nomenclature. *J Biol Chem*. 2001;276(36):33293–33296.
15. Schechter I, Berger A. On the size of the active site in proteases. I. Papain. *Biochem Biophys Res Commun*. 1967;27(2):157–162.
16. Guo PC, et al. Structural insights into the unique inhibitory mechanism of the silkworm protease inhibitor serpin18. *Sci Rep*. 2015;5:11863.
17. Huntington JA, Read RJ, Carrell RW. Structure of a serpin-protease complex shows inhibition by deformation. *Nature*. 2000;407(6806):923–926.
18. Khan MS, et al. Serpin inhibition mechanism: a delicate balance between native metasta-

ble state and polymerization. *J Amino Acids*. 2011;2011:606797.
19. Lomas DA, Evans DL, Finch JT, Carrell RW. The mechanism of Z alpha 1-antitrypsin accumulation in the liver. *Nature*. 1992;357(6379):605–607.
20. Davis RL, et al. Familial dementia caused by polymerization of mutant neuroserpin. *Nature*. 1999;401(6751):376–379.
21. Tsutsui Y, Kuri B, Sengupta T, Wintrode PL. The structural basis of serpin polymerization studied by hydrogen/deuterium exchange and mass spectrometry. *J Biol Chem*. 2008;283(45):30804–30811.
22. Lomas DA, Mahadeva R. Alpha1-antitrypsin polymerization and the serpinopathies: pathobiology and prospects for therapy. *J Clin Invest*. 2002;110(11):1585–1590.
23. Madsen DE, Hansen S, Gram J, Bygum A, Drouet C, Sidelmann JJ. Presence of C1-inhibitor polymers in a subset of patients suffering from hereditary angioedema. *PLoS One*. 2014;9(11):e112051.
24. Kaplan AP, Ghebrehiwet B. The plasma bradykinin-forming pathways and its interrelationships with complement. *Mol Immunol*. 2010;47(13):2161–2169.
25. Nussberger J, Cugno M, Amstutz C, Cicardi M, Pellacani A, Agostoni A. Plasma bradykinin in angio-oedema. *Lancet*. 1998;351(9117):1693–1697.
26. Wouters D, Wagenaar-Bos I, van Ham M, Zeerleder S. C1 inhibitor: just a serine protease inhibitor? New and old considerations on therapeutic applications of C1 inhibitor. *Expert Opin Biol Ther*. 2008;8(8):1225–1240.
27. Prada AE, Zahedi K, Davis AE. Regulation of C1 inhibitor synthesis. *Immunobiology*. 1998;199(2):377–388.
28. Cicardi M, Igarashi T, Rosen FS, Davis AE. Molecular basis for the deficiency of complement 1 inhibitor in type I hereditary angioneurotic edema. *J Clin Invest*. 1987;79(3):698–702.
29. Kramer J, Rosen FS, Colten HR, Rajczy K, Strunk RC. Transinhibition of C1 inhibitor synthesis in type I hereditary angioneurotic edema. *J Clin Invest*. 1993;91(3):1258–1262.
30. Basiji DA, Ortyn WE, Liang L, Venkatachalam V, Morrissey P. Cellular image analysis and imaging by flow cytometry. *Clin Lab Med*. 2007;27(3):653–670.
31. Kramer J, Katz Y, Rosen FS, Davis AE, Strunk RC. Synthesis of C1 inhibitor in fibroblasts from patients with type I and type II hereditary angioneurotic edema. *J Clin Invest*. 1991;87(5):1614–1620.
32. Staunstrup NH, et al. Development of transgenic cloned pig models of skin inflammation by DNA transposon-directed ectopic expression of human β1 and α2 integrin. *PLoS One*. 2012;7(5):e36658.
33. Osler W. Landmark publication from The American Journal of the Medical Sciences: hereditary angio-neurotic oedema. 1888. *Am J Med Sci*. 2010;339(2):175–178.
34. Donaldson VH, Evans RR. A biochemical abnormality in herediatry angioneurotic edema: absence of serum inhibitor of C' 1-esterase. *Am J Med*. 1963;35:37–44.
35. Ernst SC, Circolo A, Davis AE, Gheesling-Mullis K, Fliesler M, Strunk RC. Impaired production of both normal and mutant C1 inhibitor proteins in type I hereditary angioedema with a duplication in exon 8. *J Immunol*. 1996;157(1):405–410.
36. Verpy E, et al. Crucial residues in the carboxy-terminal end of C1 inhibitor revealed by pathogenic mutants impaired in secretion or function. *J Clin Invest*. 1995;95(1):350–359.
37. Miranda E, Römisch K, Lomas DA. Mutants of neuroserpin that cause dementia accumulate as polymers within the endoplasmic reticulum. *J Biol Chem*. 2004;279(27):28283–28291.
38. Yazaki M, et al. Biochemical characterization of a neuroserpin variant associated with hereditary dementia. *Am J Pathol*. 2001;158(1):227–233.
39. Mahadeva R, et al. Heteropolymerization of S, I, and Z alpha1-antitrypsin and liver cirrhosis. *J Clin Invest*. 1999;103(7):999–1006.
40. Roche O, Blanch A, Duponchel C, Fontán G, Tosi M, López-Trascasa M. Hereditary angioedema: the mutation spectrum of SERPING1/C1NH in a large Spanish cohort. *Hum Mutat*. 2005;26(2):135–144.
41. Si-Tayeb K, et al. Highly efficient generation of human hepatocyte-like cells from induced pluripotent stem cells. *Hepatology*. 2010;51(1):297–305.
42. Takayama K, et al. Prediction of interindividual differences in hepatic functions and drug sensitivity by using human iPS-derived hepatocytes. *Proc Natl Acad Sci U S A*. 2014;111(47):16772–16777.
43. Maguire AM, et al. Age-dependent effects of RPE65 gene therapy for Leber's congenital amaurosis: a phase 1 dose-escalation trial. *Lancet*. 2009;374(9701):1597–1605.
44. Hacein-Bey-Abina S, et al. Efficacy of gene therapy for X-linked severe combined immunodeficiency. *N Engl J Med*. 2010;363(4):355–364.
45. Nathwani AC, et al. Adenovirus-associated virus vector-mediated gene transfer in hemophilia B. *N Engl J Med*. 2011;365(25):2357–2365.
46. Qiu T, et al. Gene therapy for C1 esterase inhibitor deficiency in a murine model of hereditary angioedema [published online ahead of print July 30, 2018]. *Allergy*. https://doi.org/10.1111/all.13582.